



# Treball Final de Grau

**Inverse Size-Exclusion Chromatography (ISEC) set-up for  
porosimetry characterization of acidic ion-exchange resins.**

Albert Miró i Rovira

*June 2019*



UNIVERSITAT DE  
BARCELONA



Aquesta obra està subjecta a la llicència de:  
Reconeixement–NoComercial–SenseObraDerivada



<http://creativecommons.org/licenses/by-nc-nd/3.0/es/>



*The aim of natural science is not simply to accept the statements of others, but to investigate the causes that are at work in nature.*

Albert of Lauingen

Primer de tot, agrair als meus tutors, la Dra. Ramírez i el Dr. Soto, tot l'immens esforç que han fet per fer possible la realització d'aquest treball. La Dra. Ramírez que ha hagut d'ensenyar-me tot el funcionament del laboratori i els equips des del principi. I el Dr. Soto que fins i tot ha invertit el seu temps de lleure i moltes hores durant aquest any en mi i aquest treball.

En segon lloc, agrair a tots els professors del grup de Cinètica Aplicada i Catàlisi que m'han ajudat en la realització d'aquest treball, el Dr. Badia, el Dr. Bringué, el Dr. Cunill, el Dr. Fité, la Dra. Iborra i el Dr. Tejero.

Per últim, agrair a tota la meva família el suport, els ànims i els consells que m'han donat durant tota la meva carrera acadèmica i en especial durant la realització d'aquest treball. Sense ells no hauria arribat on sóc avui.



# CONTENTS

|   |            |
|---|------------|
| <b>SUMMARY</b>  | <b>i</b>   |
| <b>RESUM</b>  | <b>iii</b> |
| <b>1. INTRODUCTION</b>  | <b>1</b>   |
| <b>1.1. FOSSIL FUELS</b>  | <b>1</b>   |
| 1.1.1. Worldwide situation  | 1          |
| 1.1.2. Gasoline   | 4          |
| 1.1.3. Gasoline engine behaviour (Knocking)   | 4          |
| 1.1.4. Emissions from gasoline usage  | 4          |
| <b>1.2. GASOLINE REFORMULATION</b>  | <b>5</b>   |
| 1.2.1. Oxygenates   | 6          |
| 1.2.2. Evolution of oxygenates usage  | 7          |
| <b>1.3. ETHYL TERT-BUTYL ETHER (ETBE)</b>   | <b>8</b>   |
| 1.3.1. Properties of ETBE   | 8          |
| 1.3.2. Synthesis of ETBE  | 8          |
| <b>1.4. ION EXCHANGE RESINS (IERS) AS CATALYSTS</b>                                       | <b>9</b>   |
| 1.4.1. Synthesis of polystyrene divinylbenzene resins (PS-DVB)                            | 10         |
| 1.4.2. Acidic Ion Exchange Resins (Sulfonated IERS)                                       | 12         |
| 1.4.3. Catalytic activity and accessibility of sulfonic polystyrene divinylbenzene resins | 13         |
| <b>1.5. ISEC (INVERSE SIZE EXCLUSION CHROMATOGRAPHY)</b>                                  | <b>15</b>  |
| 1.5.1. Scientific fundamentals  | 15         |

---

|   |           |
|---|-----------|
| 1.5.2. Calculus and system modelling  | 17        |
| <b>1.6. STATE OF THE ART</b>  | <b>18</b> |
| <b>2. OBJECTIVES</b>  | <b>23</b> |
| <b>3. EXPERIMENTAL PROCEDURE</b>  | <b>25</b> |
| <b>3.1. MATERIALS</b>   | <b>25</b> |
| 3.1.1. Chemicals  | 25        |
| 3.1.2. Catalysts  | 26        |
| <b>3.2. EXPERIMENTAL SETUPS</b>   | <b>27</b> |
| 3.2.1. Gravity column packing setup   | 27        |
| 3.2.2. Suction column packing setup   | 28        |
| 3.2.3. ISEC setup   | 29        |
| <b>3.3. EXPERIMENTAL PROCEDURE</b>  | <b>30</b> |
| <b>3.4. DATA PROCESSING</b>   | <b>32</b> |
| 3.4.1. Obtaining the elution volume   | 32        |
| 3.4.2. Data processing with the software  | 32        |
| <b>4. RESULTS</b>   | <b>37</b> |
| <b>4.1. COMPARISON OF THE VALUES BETWEEN EXPERIMENTS OF THE SAME RESIN</b>  | <b>37</b> |
| <b>4.2. COMPARISON OF THE VALUES BETWEEN THE EXPERIMENTS OF THIS PROJECT AND REFERENCE VALUES</b>   | <b>39</b> |
| <b>4.3. EVALUATION OF THE EFFECT OF CHANGES IN MODELLING PARAMETERS: KINETIC DIAMETER , MACROPORE LIMIT AND CHAIN DIAMETER TO THE EXPERIMENTAL CHARACTERIZATION OF RESINS</b> | <b>43</b> |
| <b>4.4. EVALUATION OF THE RELATIONSHIP BETWEEN CATALYTIC ACTIVITY AND MORPHOLOGICAL PROPERTIES</b>  | <b>45</b> |
| <b>5. CONCLUSIONS</b>   | <b>47</b> |



|                                       |           |
|---------------------------------------|-----------|
| <b>REFERENCES AND NOTES</b>           | <b>49</b> |
| <b>ACRONYMS</b>                       | <b>51</b> |
| <b>APPENDICES</b>                     | <b>55</b> |
| <b>APPENDIX 1: VALUES FOR FIGURES</b> | <b>57</b> |



## **SUMMARY**

This project covers the implementation and application of the technique Inverse Steric Exclusion Chromatography (ISEC) for the characterization of several types of ion-exchange resins. Among many other uses, these catalysts are widely applied for etherification and esterification reactions where the presence of alcohols provides the polar media that causes the resins swelling. The novelty of ISEC relies on the feasibility for characterizing the polymers in the swollen state and therefore allowing for a better description of the catalysts actual reaction working state. A set of ion-exchange resins of different properties will be characterized using the previously implemented technique and their morphology will be discussed according to the experimental results. The assessment of the reproducibility achieved and the influence of important parameters used in the modelling on the morphological properties derived are also main objectives for this work.

**Keywords:** Morphological characterization, Heterogeneous catalysis, ISEC, Ion-exchange resins, ETBE, Biofuels.



## RESUM

Aquest treball es centra en la implementació i aplicació de la tècnica de cromatografia inversa d'exclusió estèrica (ISEC) per a la caracterització de diversos tipus de resines de bescanvi iònic. De les moltes aplicacions que tenen aquestes resines, s'utilitzen com a catalitzadors en reaccions d'eterificació i esterificació on la presència d'alcohols proporciona el medi polar necessari que causa que les resines s'inflin. La novetat de l'ISEC es basa en la viabilitat per caracteritzar els polímers (de les resines) en un estat inflat i, per tant, permet una millor descripció en les condicions de treball dels catalitzadors. Una selecció de resines de bescanvi iònic de diferents propietats es caracteritzaran utilitzant aquesta tècnica i la seva morfologia serà estudiada d'acord amb els resultats experimentals obtinguts. La valoració de la reproductibilitat aconseguida en aquests resultats i la influència dels paràmetres més importants utilitzats en la modelització de les propietats morfològiques són també objectius d'aquest treball.

**Paraules clau:** Caracterització morfològica, catàlisi heterogènia, ISEC, Resina de bescanvi iònic, ETBE i biocombustibles.



# 1. INTRODUCTION

Our society depends mainly on non-renewable resources, like natural gas, oil and coal, to fulfil our energy and transportation needs. Apart from the obvious drawback of depending of non-renewable resources, this resources are finite and cannot be regenerated at a rate equal or superior to the rate that are being consumed. It is also important to address the current situation of the environment and climate change in part caused by the use of this resources.

## 1.1. FOSSIL FUELS

### 1.1.1. Worldwide situation

Nowadays fossils fuels are the main source that drive our transportation means. In particular, oil accounts for a large percentage of the worldwide energy consumption, ranging from 32% in Europe and Asia, to 53% in the Middle East. For other regions: 44% in South and Central America, 41% in Africa, and 40% in North America. An important part of the consumed oil is dedicated to the manufacture of transportation fuels as gasoline, diesel, fuel oil, jet fuel or kerosene [1].

As a result of the increasing consumption of these substances, the level of pollutants in the atmosphere has been increasing continuously and so the emission of harmful compounds, as greenhouse gases (GHG) [1], which raises a major global concern of paramount importance and motivates the research of alternatives. In transportation, we have to major currents: on one hand electric and hybrids cars, and in the other, alternatives fuels for the combustion engine, for example LPG, LNG and biofuels. The framework of the current is related to the latter, being of relevance for the production of greener fuels.

Electric cars have a major drawback compared to the combustion engines vehicles, they lack of the necessary infrastructure to be fully functional, and currently, recharge stations are only found inside cities, which hampers the usage of these cars between cities due to their low battery range. Also the batteries are very expensive and heavy. Moreover, the need of lithium and cobalt

to produce them implies a high environmental impact during the construction and later on for the disposal [2].

Furthermore, the major reserves of cobalt in the world are mainly found in the Democratic Republic of Congo, known for its political instability and continued warfare conflicts fuelled by the money obtained from selling metals as Niobium, Tantalum and others in mines with despicable conditions. Lithium reserves are found mainly in Australia, Chile and Argentina, which do not have the same problematic but there have been doubts about the feasibility of dealing with worldwide lithium demand for future production of lithium-ion batteries for vehicles and electronics [2].

Another lithium production issue is stated by Credit Suisse and compares the current situation of lithium with the one of oil in the near past. The demand of lithium exceeds nowadays the current production by 25% which means that prices for this material will rise until new and more expensive extraction processes are economically feasible for investors to boost the global production of lithium, similarly to the case of oil and the development of deep water and oil sands extraction techniques [3].

Also the use of lithium batteries in domestic vehicles raises a major red flag because of the fact that lithium batteries can overheat and possibly explode, in a process called thermal runaway, when short-circuited. Although most consumer lithium batteries have thermal overload protection systems to prevent this from happening, internal short-circuits from manufacturing defects or physical damage can cause a spontaneous thermal runaway, this could happen during a crash accident which would endanger the lives of the occupants and their chances of surviving.

LPG and LNG which stands for liquated petroleum gases and liquated natural gas respectively, are an alternative to main stream fuel for combustion engines. They are cleaner, in comparison with conventional fuel, by emitting less greenhouse gases when used. Although it has also major drawbacks, first of all it is still a non-renewable source, because it comes from petrol or natural gas like conventional fuels. Also like electric cars currently lacks the infrastructure necessary to be fully operational and without creating any setbacks in comparison to the current situation.



Such an analysis points biofuels out as a feasible choice to replace gasoline and diesel at least in the near future, being able to repurpose all the current infrastructure for conventional fuels and the vehicles. Meanwhile other technologies can continue developing, avoiding the dependence of a non-renewable resource and reducing the impact on the environment caused by human activity. As it can be seen in the Figure 1.1, biofuels production is increasing worldwide.

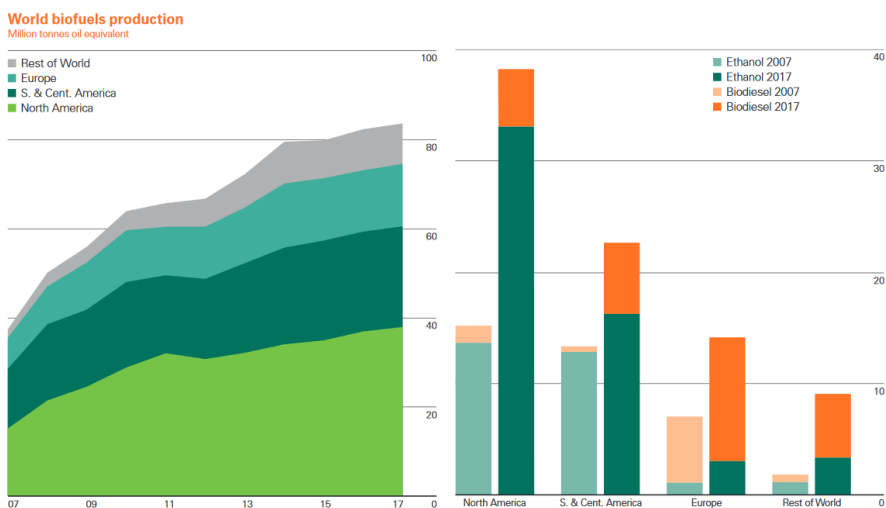


**Figure 1.1** Evolution of biofuels production in the last years (BP annual report 2017)

Two main commodities for transportation are generated from oil, gasoline and diesel. The usage of both products depends on the world region. Gasoline is mainly used in US, Brazil, Japan, Australia and the Middle East, whereas diesel is mostly used in Asia and Europe. Diesel main advantage is that emits less greenhouse gases in its combustion, approximately 15% less CO<sub>2</sub> than gasoline, but it also emits four-fold more nitrogen dioxide (NO<sub>2</sub>) and 22 times more particulate matter (PM). Accordingly, overextended use of diesel in urban environments can have fatal consequences, for example Paris in March 2016 reached pollution levels so elevated that became temporary the most polluted city in the world. In response, the government created laws to limit the usage of diesel vehicles; a ban to new diesel engines and limiting half the amount of diesel vehicles to circulate on alternated days. Moreover, in Europe some city councils are considering banning completely diesel vehicles from circulating by 2021. As a consequence of such measure, it is possible that the demand for gasoline vehicles grows in the near future [1].

### **1.1.2. Gasoline**

Gasoline is a transparent liquid obtained from the fractional distillation of petroleum and is used as a fuel for internal combustion engines. The main components of gasoline can be separated into paraffins/iso-paraffins, olefins/iso-olefins, naphthenes, and aromatics [4]. In addition, a wide variety of additives are used in fuels to add specific properties (better burning, reduction of emissions, etc.) to the fuel mixture, as oxygenates or detergents [1].

### **1.1.3. Gasoline engine behaviour (Knocking)**

When using gasoline in a combustion engine, the air/fuel mixture makes a homogenous combustion in each of the engine's cylinders after a spark induces it. When the front of the flame sweeps through the cylinder, the fuel that has not burned yet undergoes an increase in temperature due to the compression. This causes a detonation in the chamber and in consequence a brusque pressure increase. This energy released cannot be used to push the piston, because is subjected to the crankshaft, which is also connected to the other pistons. Instead, it creates a punctual strike that causes high frequency pressure fluctuations in the combustion chamber, which causes a strong metallic noise that gives name to this effect, "knocking". This knocking, apart from being a waste of energy that could have propelled the piston, it overheats the valves, spark-plugs and piston, reducing the engine's lifespan. Knocking is the end result of chemical reactions of the air/fuel mixture inside a cylinder as a consequence of the spontaneous burning of this mixture. As the temperature of the mixture rises through the cylinder during combustion, the residual gas is involved in a series of oxidation and cracking reactions that result in unstable compounds susceptible to self-ignition and instantaneous detonation [5].

### **1.1.4. Emissions from gasoline usage**

The emissions from combustion of gasolines strongly depend on the gasoline composition. For gasolines with high content of olefins and aromatic hydrocarbons, it will emit more unburned hydrocarbons, also known as volatile organic compounds (VOC). Catalytic converters found in vehicles exhaust have trouble oxidizing hydrocarbons, and if emitted to the atmosphere these substances are precursors of photochemical contamination and also represent a high danger as greenhouse effect gases. A very important property related to the emission of VOCs is the vapor

pressure of the mixture, being the emissions lower for mixtures of lower vapor pressure. Also an engine performance will perform better when the fuel volatility is lower [6].

Other pollutants that are emitted are: carbon monoxide (CO), carbon dioxide CO<sub>2</sub>, particulate matter (PM), in particular for human beings PM<sub>10</sub>, PM<sub>2.5</sub> and PM<sub>0.1</sub> known as coarse, fine and ultrafine particle matter respectively (also called inhalable, thoracic and respirable as in their ability to enter parts of the human body) and nitrogen oxides (NO<sub>x</sub>).

NO<sub>x</sub> and VOCs when released in the atmosphere react with sunlight, in photochemical reactions, that cause the formation of tropospheric ozone, which is a very toxic pollutant for human life. Also other atmospheric oxidants can be formed by gasoline vehicles, for example hydrogen peroxide, which then can react with SO<sub>2</sub> creating sulfuric acid aerosol, aldehydes, organic acids, nitric acid, and the peroxyacyl nitrates (PANs) [1].

## 1.2. GASOLINE REFORMULATION

Biofuels can be used as additives in conventional fossil fuels to reduce the derived effects from gasoline combustion. This is why many western countries have been implementing new legislation to promote fuel reformulation. Starting with replacing tetraethyl lead as an antiknock (octane rating) additive to prevent engine knocking (mainly oxygenates). Later decreasing the olefin content, increasing the content of oxygenates and reducing the blending Reid vapour pressure (bRVP) of fuels. Examples of such changes of legislation are the C.A.A.A. (Clean Air Act Amendments) in the United States of America and the Directives 2009/28/EC, 2009/30/EC and 2015/1513/EC in Europe. Furthermore, Directive 2003/96 allows European member states to apply a total or partial tax exemption to biofuels, thus making biofuel production more competitive than classical fossil fuels. Finally, refiners have a significant incentive to increase the production of reformulated gasoline and to reduce the production of conventional one [1].

Many other countries (Argentina, Colombia, India, Australia, Brazil, U.S., ...) with a large farming sector have been developing mixtures of conventional fuels (gasoline and diesel) with biofuels (bioethanol and biodiesel respectively). Ignition engines can work with mixtures of up to 25% dehydrated alcohol without modifications to the engine, but its performance varies with respect to conventional fuel. In Europe, the maximum limit for ethanol is 7.8% (Directive 2009/30/EC), a mixture of 5% ethanol normally used in some European countries.

Alternative additives to gasoline, which come from a renewable source, have also been developed, e.e.g. oxygenates as a replacement for tetraethyl lead as antiknock agents.

### 1.2.1. Oxygenates

Oxygenates compounds are chemical substances that contain oxygen, e.g. alcohols, carboxylic acids, ketones, ethers, esters and phenols among others. These substances have been gaining terrain in the gasoline making since lead compounds, as tetraethyl lead, were banned as octane enhancers due to their toxicity for humans. But only alcohols and ethers are used for gasoline production and esters for diesel.

Gasoline oxygenates are used to increase the octane rating and to add oxygen in the fuel mixture, which contributes to a more complete combustion, reducing the emissions of CO (up to 46% in weight), CO<sub>2</sub> and VOC. Also they can be used as substitutes for aromatics compounds in high performance gasoline. Their blending is also effective for eliminating the usage of carcinogenic compounds, as toluene, and reducing the emission of PM and VOC [7, 8].

Ethanol is the most used alcohol as additive in gasoline worldwide, because it is considered a renewable and green additive for gasoline since it can be obtained from fermentation of corn and other crops, algae and agricultural waste. This means that does not add more CO<sub>2</sub> in the atmosphere, because although its combustion generates CO<sub>2</sub> it is balanced due to the fact that its production cycle has been eliminating CO<sub>2</sub> before its use.

Fuel mixtures that contain ethanol have a code (EXX), where XX are numbers that are indicative of the volumetric percentage of ethanol in the mixture, e.g. E85 is a blend that contains 85% anhydrous ethanol and 15% gasoline. Low ethanol-blends, also named gasohol, which only contain 25% of ethanol can be used in conventional engines. Blends of 10% or less ethanol (E10) are used widespread in Europe and other countries, being the biggest user the United States of America. In Brazil higher blending mixtures are typically used like E20 and E25. E85 is very used in the U.S., and with less extend in Europe, using Flexible Fuel Vehicles (FFVs). E100 is used in Brazil on neat ethanol vehicles and FFVs and hydrous E15 in the Netherlands. Furthermore, in recent years heavier alcohols as butanol are being considered as potential additives for gasoline blends, because it can be obtained by fermentation from renewable carbohydrate substrates [9].

Methyl *tert*-butyl ether (MTBE), ethyl *tert*-butyl ether (ETBE), *tert*-amyl methyl ether (TAME), and *tert*-amyl ethyl ether (TAEE) are the most produced tertiary ethers as oxygenates worldwide.

All these are made of the addition of primary alcohols to tertiary olefins over acidic ion exchange resins. MTBE and TAME use methanol as primary alcohol and ETBE and TAEE use ethanol instead [10].

### **1.2.2. Evolution of oxygenates usage**

As mentioned, ethanol has a clear limitation due to its oxygen content. Consequently, mainly ethers (MTBE, ETBE, TAME and TAEE) have been developed as additives to conventional fuels in Europe.

Although MTBE had recently seen an uptick in its production (since 1979 in the U.S.) as a gasoline additive for its blending characteristics and low cost, nowadays its production in the western countries has been continually decreasing due to environmental issues. Mainly the persistence of MTBE or chemical mixtures with MTBE in groundwater reserves and aquifers and the appearance of methanol in tailpipe emissions of ignition vehicles [11].

The U.S. legislation ordered to replace MTBE as a fuel additive moving back to ethanol. In Europe, other etherification products like ETBE have gained more usage and market relevance. The reasoning behind this decision is that although the blending of gasoline with EtOH is better from an economic standpoint, it has some drawbacks in the technical field, e.e.g. higher vapour pressure, higher latent heat of vaporization, the risk of introducing water into the mixture (generating phase separation), lesser energetic and enthalpy of combustion than ethers. Furthermore, usage of ethanol in conventional combustion engines can create corrosion related problems and due to it is higher bRVP can cause more pollutant emissions than conventional gasoline [7,12,13]. Its higher oxygen content helps generate more NO<sub>x</sub> and raise the oxygen content of the mixture above the legal limit (the oxygen content limit in Europe is 2.7%, which means limiting the use of ethanol to 7.8% in gasoline mixtures). Lastly, the fuel consumption of EtOH mixtures is 40% higher than that of tertiary ethers mixtures [14].

## 1.3. ETHYL TERT-BUTYL ETHER (ETBE)

### 1.3.1. Properties of ETBE

Ethyl tert-butyl ether ( $C_6H_{14}O$ ) is an asymmetrical ether with six carbon atoms and the following chemical structure:

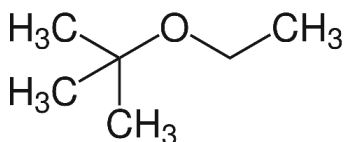


**Figure 1.2.** Scheme of an ETBE molecule (Leyo, 01/04/2007 via Wikimedia Commons, Creative Commons Attribution)

It is a colourless liquid, stable volatile and partially soluble in water at environment conditions. It is not a very biodegradable but it can be removed quite easily form the environment, in comparison with MTBE, especially from water. Like most ethers, it can form peroxides during storage and hence a stabilizer is normally added during manufacture [15].

### 1.3.2. Synthesis of ETBE

ETBE is mainly synthesized at industrial scale through the liquid-phase reaction of isobutene present in  $C_4$  streams from FCC or steam cracking (SC), with ethanol. This process is usually catalysed by ion exchange resins, in particular macroporous sulfonic acid resins at a temperature below 353 K under pressurized conditions (see Fig. 1.3). As mentioned ETBE presents better behaviour characteristics with gasoline than ethanol itself, because does not induce the evaporation of gasoline and does not absorb moisture [15].

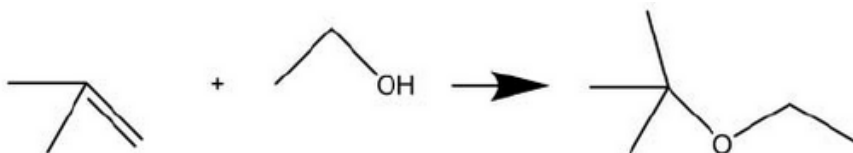


**Figure 1.3.** Scheme of the synthesis of ETBE form isobutene and ethanol (image extracted from Whelton, A. & Nguyen, T. CRIT REV ENVIRON SCI TECHNOL. 2012. 43.)

## 1.4. ION EXCHANGE RESINS (IERS) AS CATALYSTS

Ion exchange resins (IER) are solid organic substances formed by a polymeric matrix made of hydrocarbon chains with a hydrophobic character, which form a three-dimensional structure in which functional groups, with a hydrophilic character, are bonded. Depending on the nature of its functional groups IER can be classified as cationic (if functional groups are acid), anionic (if functional groups are basic) or both [1].

Due to its structure, IER are insoluble in most conventional solvents, unless a solvent can break C-C bonds. Resins have different chemical, thermal and mechanical stability depending of their chemical structure, being the most important factors their cross-linking degree and the functional groups nature [1].

IER can be classified by their morphological types as follows [16]:

- Gel-type resins. These resins do not present appreciable porosity when dry. Its interior is only accessible after swelling due to the interaction with the environment medium. (See Figure 1.4 A)
- Macroporous resins. These resins have stable macropores in the dry state, in addition to micropores when the polymer skeleton swells. (See Figure 1.4 B). They can be considered as an agglomerate of gel-type microspheres.

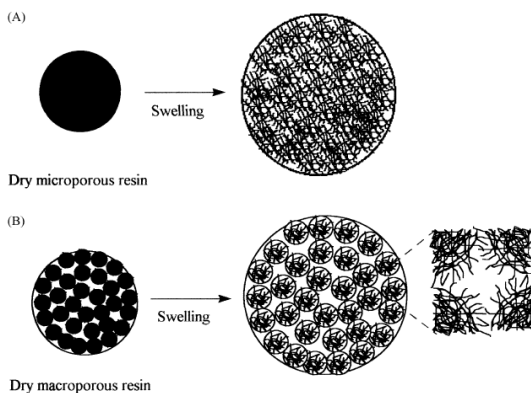


**Figure 1.4.** Scheme of a gel-type resin (A) and a macroporous resin (B) in their dry and swollen state. (Image extracted from Corain et al. *Journal of Molecular Catalysis A-chemical*. 2001. 177. 3-20.).

According to Corain et al. when a liquid medium can solvate the polymer chains of an IER, solvent molecules penetrate the polymeric matrix and constitute the gel-phase. The gel is a quasi-solution in which osmotic pressure value raises. And therefore, the polymeric chains start to stretch out and elastic forces, opposite to swelling, build up. The swelling stops when a balance between the osmotic and elastic forces is reached [16].

Hence, swelling separates the polymeric chains from each other and enhances the accessibility of the inner part of the polymeric network dramatically [16].

As a result, swelling can make available a substantial fraction of this extremely high surface for molecular species diffusing through the gel. And so, it is evident that these resins offer a potentially much greater supporting capacity than conventional rigid inorganic catalysts [16].

The active centres are found in microporous cavities within the swollen polymer matrix of either gel-type or macroreticular resins. In addition to these swelling-dependent micropores, macroreticular resins also possess macropores more or less independent of swelling [16].

Most of the interactions between molecules and the resin occur inside swollen areas instead of on macropore walls. Therefore, data on morphology or surface area realised in dry state are not very useful for correlation with the catalytic performance of the resins [16].

#### **1.4.1. Synthesis of polystyrene divinylbenzene resins (PS-DVB)**

This resins are formed by a polystyrene-divinylbenzene polymeric matrix, to which functional groups are anchored.

PS-DVB are synthesized by suspension polymerization in water, in a very controlled environment. The organic phase, made of a homogeneous mixture of styrene, divinylbenzene, and a porogenic agent (the porogenic agent will only be used to obtain a macroreticular resin), is dispersed in the aqueous one. To stabilize the macroporous morphology, the cross-linking degree needed has to be superior to 10%. Pore size, their distribution and specific surface area of the resin can vary depending on the polymerization conditions [16].

Styrene polymerization in the presence of divinylbenzene (DVB), creates a cross-linked polymer insoluble in common organic solvents. Though the crosslinking is a complex phenomenon, DVB typically acts as crosslinking agent between two linear chains of polystyrene [16]. As seen in Figure 1.5:



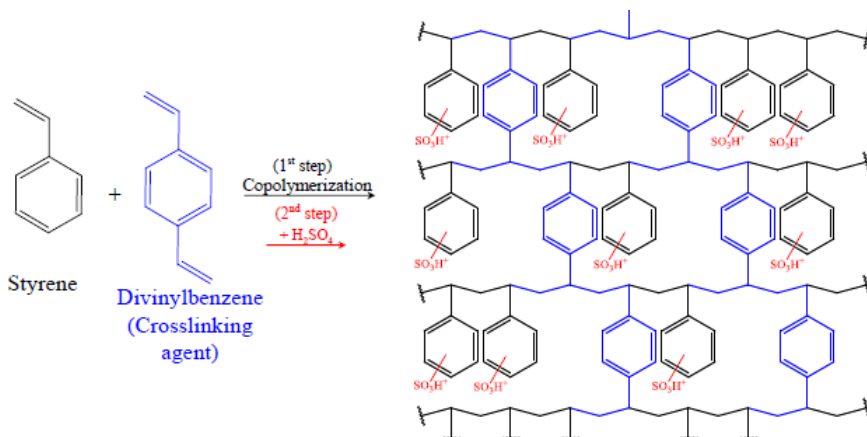


**Figure 1.5.** Scheme of the reactants to produce and acidic polystyrene divinylbenzene resin and its final structure (Image extracted Soto, R. (2017). Simultaneous etherification of C<sub>4</sub> and C<sub>5</sub> iso-olefins with ethanol over acidic ion-exchange resins for greener fuels (PhD Thesis). University of Barcelona, Barcelona.)

Microporous resins have a low crosslinking degree (DVB presence of 1-8%) with low surface areas in dry state ( $< 1 \text{ m}^2/\text{g}$ ) and without permanent porosity. Also their pores, known as micropores, are very small in size (0.7 to 2 nm) only appearing when the resin is in a liquid suspension. Instead macroporous resins have a higher crosslinking degree (DVB presence of 5-60%) and need the presence of porogens, like n-heptane, during their polymerization. In these resins pores in the region meso-macro are found. These pores are permanent and can be detected by adsorption-desorption of N<sub>2</sub> at 77 K [16]. However, permanent porosity is also influenced by swelling.

Depending of its purpose, the polymer can be functionalized using a suitable reaction with functional groups (functional groups can be acid, basic, redox or metallic complexes) or utilizing an already functionalized monomers, although the last is uncommon [17].

Acidic ion-exchange resins are usually functionalized with sulfuric acid between 90 and 140 °C. This reaction generates sulfonic groups (-SO<sub>3</sub>H) that are attached to the polymer chains, and therefore act as the functional groups giving a strongly acidic cation exchange resin (see above Fig. 1.6) [16].

This last kind of functionalized polystyrene divinylbenzene are the most widely used ones in etherification reactions due to their high catalytic activity and selectivity toward desired products.

#### 1.4.2. Acidic Ion Exchange Resins (Sulfonated IERs)

Acidic IERs have the capability, that depending on the reaction conditions, the characteristics of the environment of the swollen gel may vary between a state of liquid solution (typical of homogenous catalysts) and a solid-liquid interface state (typical of heterogeneous catalysts). This will certainly influence and modify the catalytic behaviour [16].

In an aqueous medium, IER's active catalyst is the hydroxonium cation ( $\text{H}_3\text{O}^+$ ). This cation can move freely in the vicinity of the anionic groups ( $\text{SO}_3^-$ ) that are bonded to the polymeric chains (see Figure 1.6). Although in this state the concentration of the reactant in the free solution is the determinant factor for the reaction rate, it is more important the reactant concentration inside the swollen gel cavities. Hence, in the absence of affinity between the reactant and the swollen resin, the concentration of reactant molecules inside the gel cavities will be much lower than in the free solution. This is because of steric exclusion, which depends on the reactants size and also the density of the polymeric matrix [16].

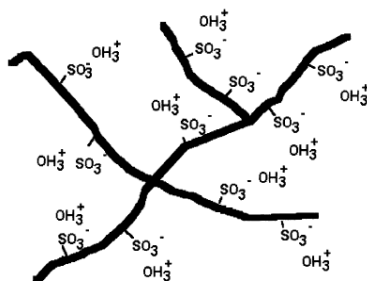


**Figure 1.6.** Scheme of the structure of an acidic IER in an aqueous environment. (Image extracted from Corain et al., *Journal of Molecular Catalysis A-chemical*. 2001. 177. 3-20.)

In non-aqueous environments or with very low concentrations of water, the active catalyst are the sulfonic groups attached to the polymeric chains (see Figure 1.7) and remain undissociated. This means, that not only the steric exclusion is a determinant factor but also the adsorption of the reactant on the polymer. Most of industrial processes involving the use of IERs use conditions for catalysis by non-dissociated acid groups [16].

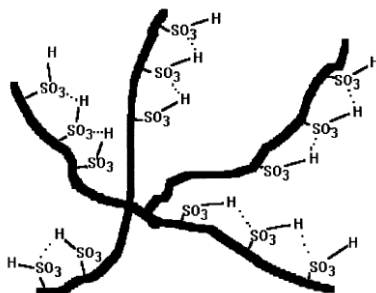


**Figure 1.7.** Scheme of the structure of an acidic IER in a non-aqueous environment. (Image extracted from Corain et al., *Journal of Molecular Catalysis A-chemical*. 2001. 177. 3-20.).

#### 1.4.3. Catalytic activity and accessibility of sulfonic polystyrene divinylbenzene resins

In a macroreticular strongly acid IER, less than 5% of the all acidic active centres are located at the macropore walls that are accessible without swelling. The remaining 95% only become accessible after contact with a liquid medium, making the polymer mass to swell and conferring additional porosity [16].

To understand the concept of accessibility, first is important to know the concept of the accessible surface area, which is the superficial area of a biomolecule that can be access by a solvent [17] as seen in Figure 1.8:

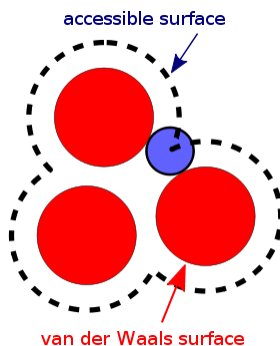


**Figure 1.8.** Scheme of how a solvent (blue) can access a biomolecule (red) by its accessible surface area (black dotted line). (Image extracted from Keith Callenberg, 06/05/2010, via Wikimedia Commons, Creative Commons Attribution)

The accessibility of the functional groups in macroreticular resins depends on the polymer chains morphology. In these materials the main role of macropores is not to provide active surface, but mainly to facilitate the contact between reactants and the resin gel phase, where most of the active centres are found. These active sites located in the cavities of the swollen polymer matrix can be understood as “microreactors” and are highly depend on its surroundings [16].

The characterization of IER in dry state are usually carried out by means of well-established methods, mainly N<sub>2</sub> adsorption-desorption, BET, nitrogen capillary condensation or mercury intrusion porosimetry. However, as discussed before, the relevance of dry state characterization of IER is not very useful since it does not allow to characterize their properties in working state (swollen) [16].

The features of swollen IER have been investigated to improve our understanding on these materials. For example, pore sizes in the swollen gel can be obtained from either the depression of the freezing point of the swelling agent (thermoporometry) or the analysis of the controlled evaporation of the swelling agent. Nevertheless, these techniques only provide us with an external picture, rather than an insightful view into their complete morphology [16].

Another useful method is the inverse steric exclusion chromatography (ISEC). It yields the best quantitative assessment of the nanomorphology of swollen IER. This technique was proposed by Halász and Freeman, it was K. Jerabeck in 1985 who firstly applied it to the characterization of swollen amorphous materials. In this method, the swollen resin is packed in a liquid chromatographic column as the stationary phase. Then, several solutes (of known molecular size) are eluted through the column governed by steric (entropic) factors only [16]. Afterwards, the elution volumes measured are related to the solid/bulk partition coefficients and the examined pore volume of different regions of the solid [16].

The data obtained by ISEC requires a mathematical treatment to provide useful information about pore volume distribution and pore sizes of the swollen resins. The following assumptions are necessary [16]:

- a) The pore system can be described using simple geometric models.
- b) It can be modelled as a discrete set of fractions, each consisting of simple pores of a single size only.

The macropores found in macroreticular resins can be described using the cylindrical pore model (to obtain pore diameter and volume). However, using the cylindrical pore model to characterize the micropores found in swollen resins resulted in unrealistic morphological parameters. Hence, the model developed by Ogston is used to characterize the gel phase. In this model, pores are defined as spaces in between randomly oriented rigid rods and it renders a better approximation for the three dimensional polymer matrix than the one obtained by the cylindrical pore model [16].

For the Ogston model, pore size is the total rod length per unit of volume, in other words the polymer chain concentration. The output of the ISEC technique is composed of the distribution pattern of the macropores, if any, and the volume distribution of the different gel fractions, classified by their density, in the swollen polymeric matrix [16].

In conclusion, the ISEC method provide a quantitative description of the morphology of a resin in the swollen state, which is more representative of the actual working state of these catalysts in reactions where polar media is induced by the presence of water or alcohols [16].

## 1.5. ISEC (INVERSE SIZE EXCLUSION CHROMATOGRAPHY)

### 1.5.1. Scientific fundamentals

This technique is used to obtain information about a material used as the stationary phase in a chromatographic column minimizing as much as possible the enthalpic interactions. The pore volume and surface area distributions can be obtained using a mathematical treatment of the elution volumes of a series of solutes of known molecular size [18].

According to Freeman and Poinescu, the structural parameters of the porous materials can be obtained by the dependence of the distribution coefficient, also known as the equilibrium partition constant ( $K$ ) with the solute molecular size [19].  $K$  is the quotient between the concentration of the solute inside the pore and in the mobile phase. The relation of  $K$  and the elution data of a solute  $j$  can be seen in Equation 1.

$$V_{e,j} = V_0 + K_j V_p \quad (1)$$

Where  $V_{e,j}$  is the elution volume of solute  $j$ ,  $V_0$  is the dead volume of the chromatographic column (the volume of the interstitial space inside the column),  $V_p$  is the pore volume and  $K_j$  is the partition constant of the solute  $j$ .

Obtaining  $V_0$  experimentally is rather simple since it corresponds to the elution volume of a solute totally excluded.

According to K. Jeřábek obtaining the value of  $V_p$  is of utmost importance for solving equation 1. The  $K$  in a porous system made of identical pores is quite simple to calculate, but when the system has non-uniform pores, its calculation becomes a challenge. To overcome this issue, a numerical approximation is proposed instead of the analytical solution. A set of a finite number of pore discrete fractions, each one of simple pores of the same size. The elution volume of a solute  $j$  with a characteristic size  $L$  in a porous system composed of  $n$  fractions is described by equation 2:

$$V_{e,j} = V_0 + \sum_{i=1}^n K_j^i(L) V_p^i \quad (2)$$

Where  $K_i(L)$  is the partition coefficient of a solute  $j$  in a fraction  $i$  of pore volume  $V_p^i$ . A key restriction in this equation is the number of solutes ( $K$ ) has to be greater or equal to the number of fractions  $n$  ( $n \leq K$ ).

The pore characteristic dimension ( $d_p$ ) for each fraction  $i$  of the  $n$  totals has to have been chosen previously as a scale for the described porous system to be real. The evaluation of the porous material is essentially the determination of the individual fractions volumes  $V_p^i - V_p^n$ . The value of  $d_p$  for a porous system can be assumed in function of the  $L$  characteristic of the molecules. It has been proved that the following values,  $d_p = 1.5L$ ,  $d_p = 2L$  and  $d_p = 2.5L$ , are the most appropriate, according to the kinetic diameter of the molecules, for a spherical molecule. From previous experimental studies of K. Jeřábek,  $d_p = 2L$  has been considered to be the most accurate [20].

As explained before, there are two types PS-DVB resins, gel-type and macroreticular. On one hand, gel-type resins do not have any true pores and their characterization only uses the Ogston model. On the other hand, macroreticular resins present true pores (meso and macro) and gel phase. Therefore, the Ogston model is used for the characterization of the gel regions, and the cylindrical pore model, for the regions of permanent porosity.

For microporous resins, the volume of the gel phase has been modelled in 5 fractions of different characteristic density of polymer chain concentration of 0.1, 0.2, 0.4, 0.8 and

1.5 nm·nm<sup>-3</sup> where the space between polymeric chains are equivalent to the pore diameters of 9.8, 4.3, 2.6, 1.5 and 1 nm, respectively. For the evaluation of the true pores, the cylindrical pore model is used to model different regions of pore diameters larger than 10 nm.

The distribution coefficient  $K_c$  for spherical molecules with diameter  $d_s$  in a system of cylindrical pores of diameter  $d_p$  can be described in equation 3:

$$K_c = (1 - d_s/d_p)^2 \quad (3)$$

This equation is only valid while  $d_s \leq d_p$ . If  $d_s > d_p$ , then  $K_c = 0$ . Also, molecules can only be considered spherical, for the rest of cases the characteristic dimension  $L$  could be a crude approximation.

For the gel phase description using the Ogston model, the partition coefficient  $K_0$  can be obtained by equation 4:

$$K_0 = \exp(-0.25\pi C(d_s + d_c)^2) \quad (4)$$

Where  $C$  is the chain density of the gel phase polymer (0.1-1.5 nm·nm<sup>-3</sup>).  $K_0$  indicates the amount of total volume of the porous system that is accessible to spherical objects of a diameter  $d_s$ . The  $d_c$ , diameter of the randomly orientated cylindrical bars, depends on the material used. With respect to the polymer chains of PS-DVB resins their value ranges from 0.3-0.5 nm. The results obtained by K. Jeřábek [20] indicate that the most appropriate value to describe the experimental results was  $d_c = 0.4$  nm.

It is important to note, that in the cylindrical pore model  $K_c$  indicates the relative accessibility of the pore volume alone. Otherwise for the Ogston model  $K_0$  it refers to the sum of the occupied volume by the free space and the volume occupied by the polymeric skeleton.

If the  $K_0$  value is wanted to be representative of the quotient between the concentration of the solute inside the pore and in the mobile phase a modification to equation 4 is needed (see equation 5).

$$K'_0 = K_0 / (1 - (\frac{\pi C d_c^2}{4})) \quad (5)$$

### 1.5.2. Calculus and system modelling

The boundary between the gel phase and the macroporous phase has been established at 8-10 nm, as K. Jeřábek suggested previously.

Using equations 3 and 4 the matrixes of  $K_c$  and  $K_0$  can be build. These matrixes have to be build according to the molecular weight and characteristic dimension of the solutes used in the ISEC experiments (these values can be found at the Experimental procedure).

For the macropouros model, only the  $K_c$  values corresponding to the dextrans are considered. As an example, the elution volume equation for Dextrane 1,500 (a solute used) is:

$$\begin{aligned}
 V_{e,D1500} = & K_{c,D1500}^{dp=4.3} V_p^{dp=4.3} + K_{c,D1500}^{dp=8.08} V_p^{dp=8.08} + K_{c,D1500}^{dp=10.22} V_p^{dp=10.22} + \\
 & K_{c,D1500}^{dp=13.24} V_p^{dp=13.24} + K_{c,D1500}^{dp=19.36} V_p^{dp=19.36} + K_{c,D1500}^{dp=25.06} V_p^{dp=25.06} + \\
 & K_{c,D1500}^{dp=30.88} V_p^{dp=30.88} + K_{c,D1500}^{dp=40.68} V_p^{dp=40.68} + K_{c,D1500}^{dp=62.06} V_p^{dp=62.06} + \\
 & K_{c,D1500}^{dp=117.58} V_p^{dp=117.58} + V_0 \quad (6)
 \end{aligned}$$

The gel phase modelling uses data from both the macropouros model and from the Ogston model. As an example, the corresponding equation for the elution of deuterium oxide solute is:

$$\begin{aligned}
 V_{e,D2O} = & K_{0,D2O}^{0.1} V_p^{0.1} + K_{0,D2O}^{0.2} V_p^{0.2} + K_{0,D2O}^{0.4} V_p^{0.4} + K_{0,D2O}^{0.8} V_p^{0.8} + K_{0,D2O}^{1.5} V_p^{1.5} + \\
 & K_{C,D2O}^{M1} V_p^{M1} + K_{C,D2O}^{M2} V_p^{M2} + \dots + K_{C,D2O}^{M,n} V_p^{M,n} + V_0 \quad (7)
 \end{aligned}$$

The first zone to consider of the macroporous dominion, M1, is defined by the molecule that needs a minimum pore diameter to pass of 10 nm. This limit is established to separate the gel phase from the macropouros phase. And as mentioned, its value ranges 8-10 nm according to the studies of K. Jeřábek. No information has been found regarding the reasons of using 8 or 10 nm. As a consequence, only the rational evaluation of the predicted data using one or another value is the method of choice.

At this point, a set of theoretical elution volume equations for each solute used, similar to Eqs. 6 and 7, are constructed. Then, the pore volume of each of the modelled fractions are obtained by minimization of the theoretical and experimental elution volumes. Using these data obtained, surface area and pore diameter can also be obtained, as well as the true volume of swollen polymer ( $V_{sp}$ ) of the total length of the polymer chains.

## 1.6. STATE OF THE ART

During the decades of 1980 and 1990, there several techniques were developed in order to approach and solve the problem with the characterization of polymers in a swollen state. These techniques based on physic-chemical methods are listed in Table 1.1 [16].



**Table 1.1.** Classification of various methods applied to swollen polymer characterization

| Method                            | Information  |
|-----------------------------------|--|
| Diffraction <sup>a</sup>          | Nanoscopic morphology  |
| ESR of paramagnetic probes        | Accessibility <sup>b</sup> , mobility <sup>b</sup>                           |
| NMR of confined solvent           | Accessibility <sup>b</sup> , mobility <sup>b</sup>                           |
| ISEC                              | Size and volume of 'pores', surface area                                     |
| X-ray microprobe analysis         | Distribution of functional groups  |
| ESR of paramagnetic probes + ISEC | Swollen state morphology, accessibility <sup>b</sup> , mobility <sup>b</sup> |

<sup>a</sup> Light, neutrons and X-ray. <sup>b</sup> Swelling solvent or dispersed probes

Molecular accessibility of an IER can be estimated by X-ray microprobe analysis (XRMA). For the use of this method polystyrene millimeter-sized particles were chloromethylated and after they were functionalized with phosphino groups. Later the rhodium (I) complexes were added in order to react with the phosphinated material. The accessibility of the molecular matter was estimated from the distribution of chlorine, phosphorus and rhodium atoms inside of the polymeric particles after each step with the XRMA method. As the cross-linking degree increased, less was the penetration in the particle of the reacting species. This technique was also applied to the sulfonation stage in the preparation of acidic IERs. The XRMA showed that the more accessible parts of the resin are sulfonated first, and later the denser polymeric regions follow. Consequently, catalytic performance test results can be correlated to the acidic centres accessibility thought to their location inside the resin [21, 22].

The diffraction technique has been used to study the heterogeneous nature of co-poly(N,N-dimethylacrylamide/methylenebisacrylamide)s gels [23].

ESR spectroscopy has been used to determine molecular mobility in swollen IERs by utilizing paramagnetic probes into the swollen gels. For the molecular probes stable nitroxide radicals and transition metal ions with unpaired electrons have been taken to consideration. This method applied to microporous material was developed by Regen in 1975. Later, Watanabe et al. introduced the concept of critical volume to explain the effects of the confinement of hydrated Cu<sup>2+</sup> ions inside of polymeric gels. The critical volume is the minimal volume of solution required for free molecular motion of solutes. For example, the critical volume for a single hydrated Cu<sup>2+</sup> ion is  $8 \pm 1.2 \text{ nm}^3$ , that is to say that, when the size of the cavities inside the polymeric gel have a lesser volume than the critical, molecular mobility in the solution is severely hindered. Through

ESR experiments with an aqueous solution of  $\text{Cu}^{2+}$  dispersed inside poly(N,N-dimethylacrylamide) gel, the mobility is lost in the 0.6 nm cavities [24].

NMR spectroscopy can also be used to obtain valuable information about the swelling medium. For example, the viscosity of toluene was observed to be 50 times higher when inside of polymeric material than in a bulk solution [25]. The experiments were realized using a PS-DVB resin functionalized with alkyl phosphonium cations, which have an application as phase transfer catalyst [26].

The ISEC method can be used to analyse the chemistry of the functionalized resins in swollen state. Such characterization provides a basis for the interpretation of the differences between the catalytic behaviour of acidic ion-exchange resins and analogues molecular acids. And as a result, a quantitative description of the effects of heterogenization of the acid catalyst on its activity has been achieved. In Figure 1.9 are three schemes of the basis of each technique explain before [16]:

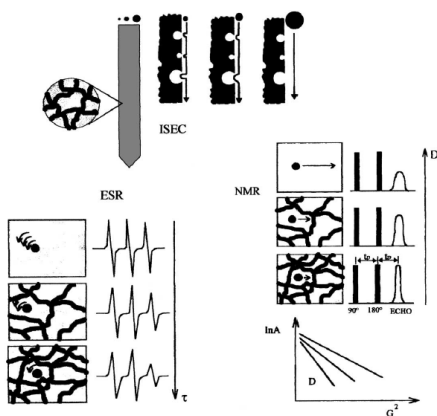


**Figure 1.9.** Scheme of how the ISEC, ESR and NMR techniques work and the signals produced by them. (Image extracted from Corain et al., *Journal of Molecular Catalysis A-chemical*. 2001. 177. 3-20.)

ISEC can also be used together with other techniques in order to achieve complementary results. Jeřábek et al. used the ISEC technique in combination with fluorescence spectroscopy to study several highly cross-linked macropores PS-DVB resins. At the same time, the BET technique was used to do the same but in the dry state. To realize the fluorescence spectroscopy a fluorescent probe was bond (using covalent bonds) to the resin structure during polymerization.

Then the resins were swollen in a series of different solvents and for each experiment, the value of  $\tau_{\max}$  of the fluorescence emission spectra was obtained. The value of  $\tau_{\max}$  depends on the solvatochromic effect (i.e. the interaction of the solvent and the solute recorded in the emission spectra). The data collected was then used to analyse the variation of the accessibility of the polymer matrix to the molecules of the swelling agent for each solvent. Finally, this investigation concluded that the accessibility of an IER depends drastically of the porogenic agent that is used during the polymerization [16].



## 2. OBJECTIVES

The main objective of this project is to evaluate the feasibility and reproducibility of the implementation of the ISEC technique in order to determine morphological properties of ion-exchange resins used as catalysts in the laboratory of Applied Kinetics and Catalysis of the University of Barcelona.

In order to assess how the morphological properties determined impact on resins catalytic performance, the etherification of isobutene with ethanol to obtain ethyl *tert*-butyl ether (ETBE) has been chosen as a model reaction.

Aiming to fulfil the main goal, a series of secondary objectives are established:

- To develop a column filling technique able to render a uniform packing of the chromatographic column based on the wet filling technique.
- To analyse various types acidic ion-exchange resins, gel-type and macroreticular resins, and how their morphological properties influence the catalytic behaviour in swollen state.
- To evaluate how the different parameters used in the pore size and distribution modelling calculations affect the morphological properties derived and to determine the optimal values for each one of them.
- To compare the obtained results with those previously reported by a reference laboratory in order to assess the degree of reliability of the implemented technique.



## **3. EXPERIMENTAL SECTION**

### **3.1. MATERIALS**

#### **3.1.1. Chemicals**

As mobile phase for the ISEC technique, an aqueous solution of sodium sulphate ( $\text{Na}_2\text{SO}_4$ ) 0.2 N was used. This solution was made with Millipore water and sodium sulphate (>99.0% GC, Sigma Aldrich, Germany).

For cleaning purposes Millipore water, and acetone (99.5% GC, PanReac AppliChem, Germany) were used for glassware. For cleaning the filters of the HPLC device used, a mixture (50% in volume) of Millipore water and Isopropyl alcohol (99.5% GC, Panreac, European Union) was used.

As mentioned, ISEC technique is based on the elution of solutes, of known characteristics. The solutes used, and their characteristics, are shown in Table 3.1:

**Table 3.1.** Solutes and their characteristics

| Solute          | MW [g/mol] | Molecular diameter (d <sub>s</sub> ) [nm] | GC [%] | Manufacturer            |
|-----------------|------------|---|--------|-------------------------|
| Deuterium Oxide | 20.03      | 0.30                                      | 99.9   | Sigma Aldrich, U.S.A.   |
| Ribose          | 150.13     | 0.57                                      | 99.0   | Sigma Aldrich, Slovakia |
| Xylose          | 150.13     | 0.78                                      | 99.0   | Sigma Aldrich, China    |
| Sucrose         | 342.30     | 1.35                                      | 99.5   | Sigma Aldrich, U.S.A.   |
| Raffinose       | 594.51     | 1.60                                      | 98.0   | Sigma Aldrich, China    |
| Dextran 1,000   | 1000.00    | 1.77                                      | -      | Sigma Aldrich, Denmark  |
| Dextran 5,000   | 5000.00    | 3.71                                      | -      | Sigma Aldrich, Denmark  |
| Dextran 12,000  | 12000.00   | 5.56                                      | -      | Sigma Aldrich, Denmark  |
| Dextran 25,000  | 25000.00   | 7.80                                      | -      | Sigma Aldrich, Denmark  |
| Dextran 50,000  | 50000.00   | 10.73                                     | -      | Sigma Aldrich, Denmark  |
| Dextran 80,000  | 80000.00   | 13.33                                     | -      | Sigma Aldrich, Denmark  |
| Dextran 150,000 | 150000.00  | 17.81                                     | -      | Sigma Aldrich, Denmark  |
| Dextran 270,000 | 270000.00  | 23.36                                     | -      | Sigma Aldrich, Denmark  |
| Dextran 410,000 | 410000.00  | 28.32                                     | -      | Sigma Aldrich, Denmark  |
| Dextran 670,000 | 670000.00  | 35.51                                     | -      | Sigma Aldrich, Denmark  |

Prior to use them for ISEC analysis, they need to be dissolved in mobile phase. In the case of the sugars 0.5 grams were added to 100 mL of mobile phase. For the Deuterium Oxide 3.6 mL were added to 100 mL of mobile phase. For dextrans, approximately 0.1 g of each were dissolved in 100 mL of mobile phase. Since these substances are hydrocarbons dissolved in water they should be kept in storage without light exposure to avoid their degradation due to the possible appearance of algae.

### 3.1.2. Catalysts

For this project, five acidic ion-exchange resins were used: Amberlyst™15 (A-15), Amberlyst™35 (A-35), Amberlyst™39 (A-39), Purolite®CT-124 (CT-124) and Purolite®CT-275 (CT-275). In Table 3.2 [1] gathers some of the main physical properties of these catalysts:



**Table 3.2.** Main properties of the catalysts

| Catalyst | Type  | Acid Capacity [eq H <sup>+</sup> ·kg <sup>-1</sup> ] <sup>a</sup> | DVB [%] <sup>b</sup> | Bead diameter (d <sub>b</sub> ) [mm] <sup>c</sup> | Moisture [%] <sup>d</sup> | Maximum Operating Temperature [°C] | Sulfonation type <sup>e</sup> |
|----------|-------|---|----------------------|---|---------------------------|------------------------------------|-------------------------------|
| A-15     | macro | 4.81  | 20                   | 0.74  | 50                        | 120                                | C                             |
| A-35     | macro | 5.36  | 20                   | 0.51  | 55                        | 150                                | O                             |
| A-39     | macro | 4.81  | 8                    | 0.54  | 60-66                     | 130                                | C                             |
| CT-124   | micro | 5   | 4                    | 0.77  | 63                        | 130                                | C                             |
| CT-275   | macro | 5.37  | high                 | 0.75  | 55                        | 145                                | O                             |

<sup>a</sup> Titration against a standard base. <sup>b</sup> Crosslinking degree classification: low (7-12%), medium (12-17%), high (17-25%), hyper (50%). <sup>c</sup> Determined by laser diffraction in air (Beckman Coulter LS particle size analyser) or manufacturer values (range). <sup>d</sup> As shipped. <sup>e</sup> Conventionally sulfonated (C), oversulfonated (O), surface sulfonated (S) and sulfonated/chlorinated (S/Cl).

For ISEC experiments, the resins particle size ( $d_p$ ) must be reduced to 0.10-0.25 mm. In such purpose, an Agate mortar and pestle were used to crush the resins and later, a set of stainless steel woven wire cloth sieves were used to separate the particles with the desired size range.

After sieving, the resins were pretreated, 20 hours in atmospheric oven at 110 °C (383.15 K) before the performance of the experiments.

## 3.2. EXPERIMENTAL SETUPS

### 3.2.1. Gravity column packing setup

At the beginning of the experimental period of this project, gravity was used to pack the chromatographic columns (using the wet filling technique). This setup, is illustrated in Figure 3.1; consisting of a glass funnel with a pipette tip attached to it. The pipette tip is introduced inside of one of the inlets of the chromatographic column and set vertically using a metallic hoop. Also a beaker is placed underneath the column to collect the excess of flowing mobile phase. To assure

a minimum level of mobile phase in the funnel, the residue tube of the ISEC setup was moved to the top of the funnel with a flow rate of 1 mL/min.

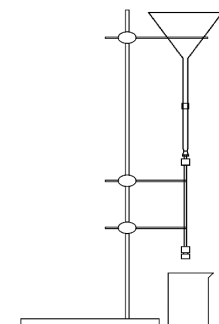


**Figure 3.1.** Scheme of the gravity column packing setup

### 3.2.2. Suction column packing setup

In this setup the main characteristic is the usage of diaphragm vacuum pump to help the column packing. Figure 3.2 plots the scheme of this setup, which essentially is the same as the gravity column packing setup (funnel (1) and chromatographic column (2)) but the exit of the column is connected to a vacuum trap (3) using a silicone pipe. A peristaltic pump (4) was used as suction device. Using this pump, the packing achieved between columns was more homogeneous in terms of mass introduced and the process of packing was significantly faster, as it will be later explained in the Experimental Procedure section.

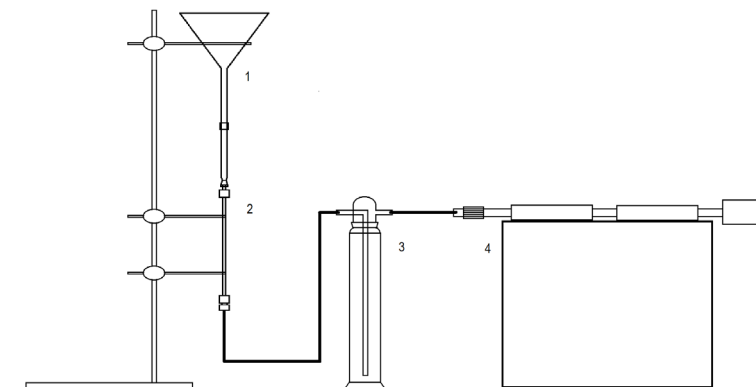


**Figure 3.2.** Scheme of the suction column packing setup

### 3.2.3. ISEC setup

The resin characterization experiments were carried out using the ISEC technique, which comprises the following setup parts: a pump, an injector, a chromatographic column and a refractive index detector (RID) detector (see Figure 3.3). A series of pulse-response experiments with all the solutes were performed to obtain the characteristic elution volumes from which the morphological properties will be obtained later on.

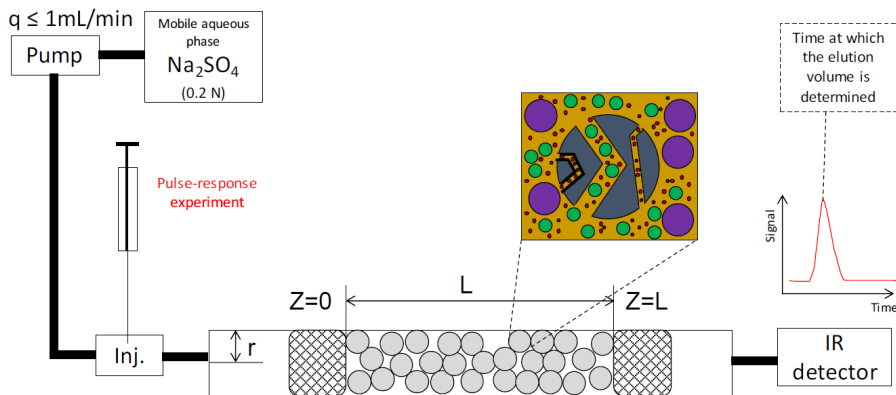


**Figure 3.3.** Scheme of the ISEC setup

In the laboratory the following equipment has been used for making the setup:

- Mobile phase storage module: Agilent Technologies 1260 Infinity.
- Isocratic Pump for ISEC: G7110B 1260 Isocratic pump, Agilent Technologies.
- Chromatographic column module: G1316A 1260 TCC, Agilent Technologies.
- Chromatographic liquid column: HPLC Column RS-25135 [250mm L x 4.6mm ID x 1/4"OD], RESTEK.
- Injection module: G1328C 1260 Manual Injector, Agilent Technologies.
- Detection module (Refractometer): G1362A 1260 RID, Agilent Technologies.

### 3.3. EXPERIMENTAL PROCEDURE

The first step for an ISEC experiment is to pack the chromatographic column with a resin using the wet filling technique. Firstly, we need to prepare a slurry of resin and mobile phase. The resin particles have a particle diameter ( $d_p$ ) between 0.10 and 0.25 mm that maintain the relations  $L/d_{column}$  and  $d_{column}/d_p$  to ensure plug flow. For the preparation of the slurry, approximately 4 grams of crushed, sieved and pretreated resin were mixed with approx. 100 ml of mobile phase in a beaker. The slurry was left approximate 30 min in stagnant conditions to assure that resin particles swell completely.

Once the slurry and the gravity column packing setup were ready, mobile phase was circulated at a flow rate between 1-2 mL/min through the empty column. With the help of a spatula, the slurry was slowly added into the funnel and then into the column by gravity. To help the packing process from time to time is convenient to hit the chromatographic column on the sides, so the slurry is compact inside and there are not void areas within the column that might lead to channelling in the subsequent part of the experiments. This process is completed when the slurry starts accumulating in the pipette tip indicating that the column is completely filled with the stationary phase (resin).

When the suction column packing setup is used to pack the chromatographic column, the procedure is slightly different. After adding the mobile phase inside the funnel on the top, the pump is switched on. Once the level of mobile phase is below the funnel, all the slurry is added into it. The pump must be running until the level of slurry in the pipette tip is constant and then switched off.

When the chromatographic column is packed with the resin, the nuts were tighten in the connection of the column to the HPLC device. Then, the oven module temperature was set to 30 °C and the RID module to 35 °C.

Once the column is connected to the HPLC, the flow rate of mobile phase was set to 0.1 mL/min. The column was let under flow conditions overnight to stabilize the base line of the RID and to ensure full ion-exchange of acidic groups, letting the resin in sodium form, minimizing therefore the possible enthalpic interactions due to the adsorption of solutes on acidic sulfonic groups.

When the base line and the pressure in the chromatographic column were stable, the pressure values were compared with those typical for an empty column (see Table 3.3) in order

to check whether the column was correctly packed avoiding possible effects of channelling. Afterwards, the flow rate was progressively increased from 0.1 to 0.6 mL/min using a flow rate gradient of 0.1 mL/min<sup>2</sup> (to avoid abrupt pressure changes that could affect the column packing).

**Table 3.3.** Column pressure values

| Flow rate [mL/min] | Pressure empty column [bar] | Pressure Column with A-35 packing [bar] |
|--------------------|-----------------------------|---|
| 0.1                | 2.1                         | 50                                      |
| 0.2                | 4.3                         | 68                                      |
| 0.3                | 6.7                         | 75                                      |
| 0.4                | 8.9                         | 84                                      |
| 0.5                | 10.1                        | 105                                     |
| 0.6                | 12.3                        | 115                                     |

When the RID base line was stable at 0.6 mL/min, the ISEC solutes were injected into the chromatographic column with a 50  $\mu$ L HPLC syringe. To avoid contamination of the solutions, a beaker with Millipore water was used to clean the syringe and the injector when changing the solute to inject. Once all the solutes have been injected, the syringe and the injector were thoroughly cleaned and Millipore water was flowed through the column (instead of mobile phase) at 1 mL/min at least for 30 min to dissolve the Na<sub>2</sub>SO<sub>4</sub> that can remain within the resin porous and can affect the subsequent weighting of the resin. After stopping the flow, the column is disconnected from the HPLC.

For extracting the resin from the column after an ISEC experiment, the column was firstly opened and, carefully, with the help of wash bottle, the slurry is extracted from the column and placed in a crucible. When all the slurry was extracted, it was dried in an atmospheric oven at 110 °C for a day. After the slurry was dried, the resin was weighed since most of the ISEC morphological properties are specific, i.e. per unit mass.

## 3.4. DATA PROCESSING

### 3.4.1. Obtaining the elution volume

The elution volume ( $V_e$ ) also known as retention volume ( $V_R$ ), is the volume of mobile phase in which the solute is eluted. The time that takes the solute from entering the chromatographic column to arrive at the RID detector is known as retention time ( $t_R$ ) (see Fig. 3.4). This retention time is crucial to obtain the elution volume using the flow rate through the column, see Equation 8.

$$V_e = Q \cdot t_R \quad (8)$$

Each solute was injected three times for obtaining averaged elution volumes and for statistical purposes about the reproducibility among injections. The value of the elution volume should be between 2 to 6 mL, either a superior or inferior value could be problematic and could be due to an incorrect column packing.

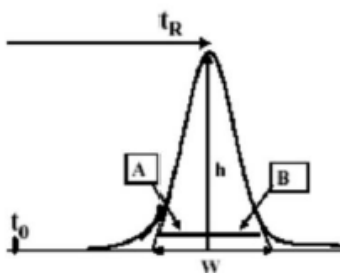
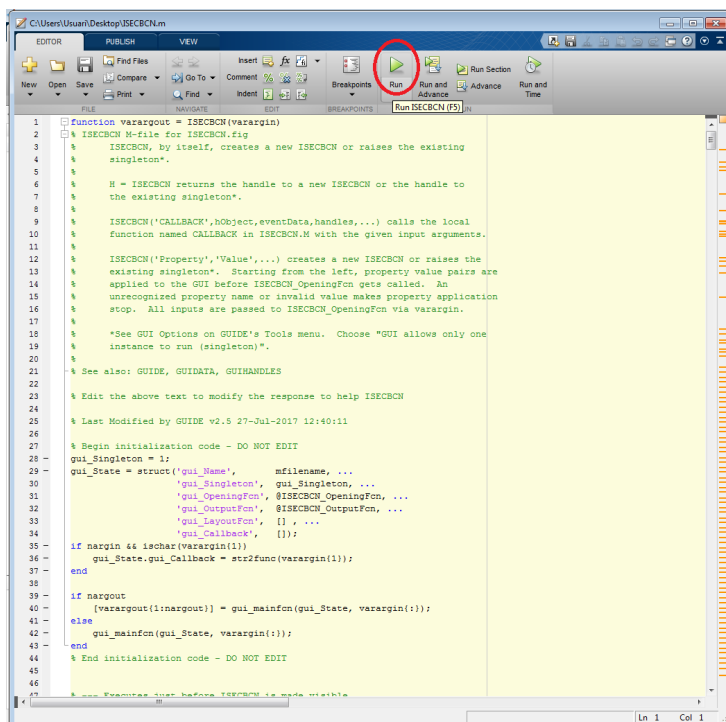


Fig 3.4. Signal obtain by the RID from an HPLC device

### 3.4.2. Data processing with the software ISECBCN

Once an ISEC experiment is finished and the elution volumes of all solutes are calculated, the process of obtaining the data of the resin morphology can be started. For this project, the data processing has been done with the program ISECBCN developed previously in our research group using the MATLAB® software.

Firstly the MATLAB® program was opened. Once there using the File menu it can be opened the ISECBCN archive. Once is opened execute the program, to do so click Run button (see the button highlighted in red in Fig. 3.5).



```
function varargout = ISECBCN(varargin)
% ISECBCN M-file for ISECBCN.fig
% ISECBCN, by itself, creates a new ISECBCN or raises the existing
% singleton*.
%
% H = ISECBCN returns the handle to a new ISECBCN or the handle to
% the existing singleton*.
%
% ISECBCN('CALLBACK', hObject,eventData,handles,...) calls the local
% function named CALLBACK in ISECBCN.M with the given input arguments.
%
% ISECBCN('Property','Value',...) creates a new ISECBCN or raises the
% existing singleton*. Starting from the left, property value pairs are
% applied to the GUI before ISECBCN_OpeningFcn gets called. An
% unrecognized property name or invalid value makes property application
% stop. All inputs are passed to ISECBCN_OpeningFcn via varargin.
%
% *See GUI Options on GUIDE's Tools menu. Choose "GUI allows only one
% instance to run (singleton)".
%
% See also: GUIDE, GUIDATA, GUIHANDLES
%
% Edit the above text to modify the response to help ISECBCN
% Last Modified by GUIDE v2.5 27-Jul-2017 12:40:11
%
% Begin initialization code - DO NOT EDIT
gui_Singleton = 1;
gui_State = struct('gui_Name',       mfilename, ...
                  'gui_Singleton',   gui_Singleton, ...
                  'gui_OpeningFcn', @ISECBCN_OpeningFcn, ...
                  'gui_OutputFcn',  @ISECBCN_OutputFcn, ...
                  'gui_LayoutFcn',  [], ...
                  'gui_Callback',    []);
if nargin && ischar(varargin{1})
    gui_State.gui_Callback = str2func(varargin{1});
end
if nargin
    [varargout{1:nargout}] = gui_mainfcn(gui_State, varargin{:});
else
    gui_mainfcn(gui_State, varargin{:});
end
% End initialization code - DO NOT EDIT
%
% Example user before ISECBCN is made visible
```

**Figure 3.5.** Window of the MATLAB® program showing the ISECBCN raw code

Once the program was executed a new window, the user interface, opened (see Figure 3.6). In this program, the user is asked to introduce the elution volumes obtained from an experiment, the flow rate, the type of resin used, diameter of the polymer chains, macropore limit boundary and kinetic diameter (F). For obtaining ISEC experiments results only the blue part of the program is needed.

**Analyze ISEC data**

| GENERAL DATA                          |                      | SPECIFIC MODELING PARAMETERS |                      |
|---------------------------------------|----------------------|------------------------------|----------------------|
| Operator Name                         | <input type="text"/> | Macropore limit (nm)         | <input type="text"/> |
| Name of porous material               | <input type="text"/> | Chain diameter (nm)          | <input type="text"/> |
| Mass of material in dry basis (g)     | <input type="text"/> | Factor (L)                   | <input type="text"/> |
| Column volume (cm <sup>3</sup> )      | <input type="text"/> | Mobile phase                 | <input type="text"/> |
| Column dead volume (cm <sup>3</sup> ) | <input type="text"/> | Mobile phase flow (mL/min)   | <input type="text"/> |

**INTRODUCE EXPERIMENTAL ELUTION VOLUMES OF THE SOLUTES USED**

|   |                      |
|---|----------------------|
| Elution volume of Deuterium Oxide (cm <sup>3</sup> )  | <input type="text"/> |
| Elution volume of Ribose (cm <sup>3</sup> )           | <input type="text"/> |
| Elution volume of Xylose (cm <sup>3</sup> )           | <input type="text"/> |
| Elution volume of Sacarose (cm <sup>3</sup> )         | <input type="text"/> |
| Elution volume of Raffinose (cm <sup>3</sup> )        | <input type="text"/> |
| Elution volume of Dextrane 1,000 (cm <sup>3</sup> )   | <input type="text"/> |
| Elution volume of Dextrane 5,000 (cm <sup>3</sup> )   | <input type="text"/> |
| Elution volume of Dextrane 12,000 (cm <sup>3</sup> )  | <input type="text"/> |
| Elution volume of Dextrane 25,000 (cm <sup>3</sup> )  | <input type="text"/> |
| Elution volume of Dextrane 50,000 (cm <sup>3</sup> )  | <input type="text"/> |
| Elution volume of Dextrane 80,000 (cm <sup>3</sup> )  | <input type="text"/> |
| Elution volume of Dextrane 150,000 (cm <sup>3</sup> ) | <input type="text"/> |
| Elution volume of Dextrane 270,000 (cm <sup>3</sup> ) | <input type="text"/> |
| Elution volume of Dextrane 410,000 (cm <sup>3</sup> ) | <input type="text"/> |
| Elution volume of Dextrane 670,000 (cm <sup>3</sup> ) | <input type="text"/> |

**Determine effective size of solutes**

**POROUS GLASS DATA**

Glass pore volume (cm<sup>3</sup>/g)

Glass pore diameter (nm)

**EXPERIMENTAL ELUTION DATA**

Solute name

Column dead volume (cm<sup>3</sup>)

Elution volume of solute (cm<sup>3</sup>)

**Determine effective dimension**

UNIVERSITAT DE BARCELONA

Developed in 2017 by Dr. Rodrigo Soto López. All the rights reserved.

**Obtain Morphological Data**

**Figure 3.6.** Window of the ISECBCN program

Once all the needed data had been inputted, the Obtain Morphological Data button was actioned. Afterwards, a Microsoft Excel<sup>®</sup> archive with the name *Iresults* comprising the morphological properties summary appeared in the desktop of the computer.

The *Iresults* file has two spreadsheets. The first one contains all the information related to the modelling of the macroporous region (see Fig. 3.7). Also the SUMMARY OF RESULTS table, where the Cumulative Pore Volume (cm<sup>3</sup>/g), the Cumulative Surface Area (m<sup>2</sup>/g), the main Pore Diameter (nm) and the sum of squared residuals are shown.



A15 2019-04-10 [Modo de compatibilidad] - Excel (Error de acti

| ARCHIVO INICIO INSERTAR DISEÑO DE PÁGINA FÓRMULAS DATOS REVISAR VISTA DESARROLLADOR |                           |  |  |             |                  |   |    |   |  |
|---|---------------------------|--|--|-------------|------------------|---|----|---|--|
| Q33   |                           |  |  |             |                  |   |    |   |  |
| A   | B                         | C  | D  | E           | F                | G | H  | I |  |
| 1 ANALYSIS INFORMATION  |                           |  |  |             |                  |   |    |   |  |
| 2 OPERATOR  | Albert                    |  | Macropore limit (nm)                       | 10.22       | DEUTERIUM OXIDE  |   | 1  |   |  |
| 3   | 11/04/2019 8:56           |  | Chain diameter                             | 0.4         | RIBOSE           |   | 2  |   |  |
| 4 Material Analysed   | A15                       |  | Factor                                     | 2           | XYLOSE           |   | 3  |   |  |
| 5 Weight of sample (g)  | 1.381                     |  | Mobile phase                               | Na2SO4      | SACAROSE         |   | 4  |   |  |
| 6 Vvol(cm <sup>3</sup> )  | 4.155                     |  | Mobile phase flow (mL/min)                 | 0.6         | RAFFINOSE        |   | 5  |   |  |
| 7 Dead volume (cm <sup>3</sup> )  | 2.042                     |  |  |             | DEXTRANE 1,000   |   | 6  |   |  |
| 8   |                           |  |  |             | DEXTRANE 5,000   |   | 7  |   |  |
| 9 GENERAL DATA  |                           |  |  |             | DEXTRANE 12,000  |   | 8  |   |  |
| 10 Solute Name  | Dimension (nm)            | Exptl. elution volume (cm <sup>3</sup> ) | Theoret. elution volume (cm <sup>3</sup> ) |             | DEXTRANE 25,000  |   | 9  |   |  |
| 11  |                           |  |  |             | DEXTRANE 50,000  |   | 10 |   |  |
| 12  | 6                         | 1.76772545                               | 2.655                                      | 2.662261702 | DEXTRANE 80,000  |   | 11 |   |  |
| 13  | 7                         | 3.712566453                              | 2.528                                      | 2.52032008  | DEXTRANE 150,000 |   | 12 |   |  |
| 14  | 8                         | 5.558661765                              | 2.411                                      | 2.407785425 | DEXTRANE 270,000 |   | 13 |   |  |
| 15  | 9                         | 7.797109934                              | 2.311                                      | 2.300336834 | DEXTRANE 410,000 |   | 14 |   |  |
| 16  | 10                        | 10.73305206                              | 2.186                                      | 2.207598122 | DEXTRANE 670,000 |   | 15 |   |  |
| 17  | 11                        | 13.33007368                              | 2.133                                      | 2.163744152 |                  |   |    |   |  |
| 18  | 12                        | 17.81145979                              | 2.184                                      | 2.133258017 |                  |   |    |   |  |
| 19  | 13                        | 23.35566701                              | 2.099                                      | 2.109053333 |                  |   |    |   |  |
| 20  | 14                        | 28.31628005                              | 2.111                                      | 2.09055207  |                  |   |    |   |  |
| 21  | 15                        | 35.51188914                              | 2.042                                      | 2.06901163  |                  |   |    |   |  |
| 22  |                           |  |  |             |                  |   |    |   |  |
| 23  |                           |  |  |             |                  |   |    |   |  |
| 24  |                           |  |  |             |                  |   |    |   |  |
| 25  |                           |  |  |             |                  |   |    |   |  |
| 26 MACROPORES MODEL BUILDING  |                           |  |  |             |                  |   |    |   |  |
| 27 Pore diam.(nm)   | Volume (cm <sup>3</sup> ) | pore volume (cm <sup>3</sup> /g)         | spec.surface (m <sup>2</sup> /g)           |             |                  |   |    |   |  |
| 28  |                           |  |  |             |                  |   |    |   |  |
| 29  |                           |  |  |             |                  |   |    |   |  |
| 30  | 3.5354509                 | 2.22045E-14                              | 1.60785E-14                                | 1.81912E-11 |                  |   |    |   |  |
| 31  | 7.425132906               | 2.22045E-14                              | 1.60785E-14                                | 8.66168E-12 |                  |   |    |   |  |
| 32  | 11.11732353               | 0.186855671                              | 0.135304613                                | 48.68244162 |                  |   |    |   |  |
| 33  | 15.59421987               | 0.389031089                              | 0.281702454                                | 72.25817173 |                  |   |    |   |  |
| 34  | 21.46510412               | 2.22045E-14                              | 1.60785E-14                                | 2.99608E-12 |                  |   |    |   |  |
| 35  | 26.66014736               | 2.22045E-14                              | 1.60785E-14                                | 2.41237E-12 |                  |   |    |   |  |
| 36  | 35.62291946               | 2.2212E-14                               | 1.6084E-14                                 | 1.80603E-12 |                  |   |    |   |  |
| 37  | 46.71137402               | 2.48377E-14                              | 1.79853E-14                                | 1.54012E-12 |                  |   |    |   |  |
| 38  | 56.6325601                | 0.194208258                              | 0.140628717                                | 9.932711248 |                  |   |    |   |  |
| 39  | 71.02377828               | 2.22046E-14                              | 1.60786E-14                                | 9.0536E-13  |                  |   |    |   |  |
| 40  |                           |  |  |             |                  |   |    |   |  |
| 41 SUM  | 0.770095018               |  | 0.557635784                                | 130.8733246 |                  |   |    |   |  |
| 42  |                           |  |  |             |                  |   |    |   |  |
| 43 SUMMARY OF RESULTS   |                           |  |  |             |                  |   |    |   |  |
| 44  |                           |  |  |             |                  |   |    |   |  |
| 45 PORE DIAM. GENERATED USING FACTOR  |                           | 2  |  |             |                  |   |    |   |  |
| 46  |                           |  |  |             |                  |   |    |   |  |
| 47 Cumulative Pore Volume (cm <sup>3</sup> /g)                                      |                           | 0.557635784                              |  |             |                  |   |    |   |  |
| 48 Cumulative Surface Area (m <sup>2</sup> /g)                                      |                           | 130.8733246                              |  |             |                  |   |    |   |  |
| 49 Pore Diameter (nm)   |                           | 24.85729899                              |  |             |                  |   |    |   |  |
| 50 Sum of Squared Errors  |                           | 0.005470996                              |  |             |                  |   |    |   |  |
| 51  |                           |  |  |             |                  |   |    |   |  |

Hoja1 Hoja2

**Figure 3.7.** Image of the spreadsheet 1 of the *Iresults* Excel archive

In the second spreadsheet there is all the information related to the modelling of the microporus region of the resin (see Fig. 3.8). Three tables can be distinguished. The first one is similar to the one found in the spreadsheet 1 with the data related to macropores (but in this case the characterisation of the macroporus region has been modified, by applying the macropore limit of 10 nm), the second one gives information about the swollen gel (Polymer concentration [nm/nm<sup>3</sup>], Volume [cm<sup>3</sup>], Pore volume [cm<sup>3</sup>/g] and the Amount of Polymer [cm/g]). In the SUMMARY OF RESULTS TABLE, a summary of the modelling results for the macro and micro regions is displayed. The Balance of Column Volume (cm<sup>3</sup>) is an important parameter since a column balance significantly different to the column real volume indicates that the modelling results are not reliable indicating therefor an incorrect packing of the column.

A15 2019-04-10 [Modo de compatibili]

ARCHIVO INICIO INSERTAR DISEÑO DE PÁGINA FÓRMULAS DATOS REVISAR VISTA DESARROLLADOR

L46 :

|    | A  | B                         | C                                | D                                | E | F |
|----|--|---------------------------|----------------------------------|----------------------------------|---|---|
| 28 |  |                           |                                  |                                  |   |   |
| 29 |  |                           |                                  |                                  |   |   |
| 30 | MACROPORES   |                           |                                  |                                  |   |   |
| 31 | Pore diam.(nm)   | Volume (cm <sup>3</sup> ) | pore volume (cm <sup>3</sup> /g) | spec.surface (m <sup>2</sup> /g) |   |   |
| 32 | -----  | -----                     | -----                            | -----                            |   |   |
| 33 |  |                           |                                  |                                  |   |   |
| 34 | 11.11732353  | 0.186855671               | 0.135304613                      | 48.68244162                      |   |   |
| 35 | 15.59421987  | 0.389031089               | 0.281702454                      | 72.25817179                      |   |   |
| 36 | 21.46610412  | 2.22045E-14               | 1.60785E-14                      | 2.99608E-12                      |   |   |
| 37 | 26.66014736  | 2.22045E-14               | 1.60785E-14                      | 2.41237E-12                      |   |   |
| 38 | 35.62291946  | 2.2212E-14                | 1.6084E-14                       | 1.80603E-12                      |   |   |
| 39 | 46.71137402  | 2.48377E-14               | 1.79853E-14                      | 1.54012E-12                      |   |   |
| 40 | 56.6325601   | 0.194208258               | 0.140628717                      | 9.932711248                      |   |   |
| 41 | 71.02377828  | 2.22046E-14               | 1.60786E-14                      | 9.05536E-13                      |   |   |
| 42 |  |                           |                                  |                                  |   |   |
| 43 | SUM  | 0.770095018               | 0.557635784                      | 130.8733246                      |   |   |
| 44 |  |                           |                                  |                                  |   |   |
| 45 |  |                           |                                  |                                  |   |   |
| 46 |  |                           |                                  |                                  |   |   |
| 47 | SWOLLEN GEL  |                           |                                  |                                  |   |   |
| 48 | Conc. Polymer(nm/nm <sup>3</sup> )                     | Volume (cm <sup>3</sup> ) | Pore volume (cm <sup>3</sup> /g) | Amount of Polymer (cm/g)         |   |   |
| 49 | -----  | -----                     | -----                            | -----                            |   |   |
| 50 | 0.1  | 2.22099E-14               | 1.60825E-14                      | 1.60825E-13                      |   |   |
| 51 | 0.2  | 2.23215E-14               | 1.61633E-14                      | 3.23265E-13                      |   |   |
| 52 | 0.4  | 0.465451493               | 0.337039459                      | 13.48157836                      |   |   |
| 53 | 0.8  | 2.22045E-14               | 1.60785E-14                      | 1.28628E-12                      |   |   |
| 54 | 1.5  | 0.442744652               | 0.320597142                      | 48.08957123                      |   |   |
| 55 |  |                           |                                  |                                  |   |   |
| 56 |  |                           |                                  |                                  |   |   |
| 57 | SUMAMRY OF RESULTS                                     |                           |                                  |                                  |   |   |
| 58 | -----  |                           |                                  |                                  |   |   |
| 59 | MACROPORES   |                           |                                  |                                  |   |   |
| 60 | -----  |                           |                                  |                                  |   |   |
| 61 | Cumulative Pore Volume (cm <sup>3</sup> /g)            | 0.557635784               |                                  |                                  |   |   |
| 62 | Cumulative Surface Area (m <sup>2</sup> /g)            | 130.8733246               |                                  |                                  |   |   |
| 63 | Pore Diameter (nm)                                     |                           | 17.04352774                      |                                  |   |   |
| 64 | Sum of Squared Errors                                  | 0.005470996               |                                  |                                  |   |   |
| 65 | GEL PHASE  |                           |                                  |                                  |   |   |
| 66 | -----  |                           |                                  |                                  |   |   |
| 67 | Chain diameter (nm)                                    | 0.4                       |                                  |                                  |   |   |
| 68 | Cumulative Swollen polymer volume (cm <sup>3</sup> /g) | 0.657636601               |                                  |                                  |   |   |
| 69 | True Swollen Polymer Volume (cm <sup>3</sup> /g)       | 0.972414903               |                                  |                                  |   |   |
| 70 | Total Length of Polymer Chains (cm/g)                  | 61.57114959               |                                  |                                  |   |   |
| 71 | Average Polymer concentration (nm/nm <sup>3</sup> )    | 0.936248827               |                                  |                                  |   |   |
| 72 | Balance of Column Volume (cm <sup>3</sup> )            | 3.720291164               |                                  |                                  |   |   |
| 73 | Sum of Squared Errors                                  | 0.029643821               |                                  |                                  |   |   |
| 74 |  |                           |                                  |                                  |   |   |
| 75 |  |                           |                                  |                                  |   |   |
| 76 |  |                           |                                  |                                  |   |   |
| 77 |  |                           |                                  |                                  |   |   |
| 78 |  |                           |                                  |                                  |   |   |

Hoja1 **Hoja2** (+)

Figure 3.8. Image of the spreadsheet 2 of the *lresults* Excel archive

## 4. RESULTS

As indicated in the objectives of this project, in order to assess the results obtained from the experiments, the following comparisons will be performed:

1. The results obtained from different experiments of the same resin, to be able to observe the reproducibility between analysis.
2. The comparison of the obtained results for different resins to those determined at the Institute of Chemical Process Fundamentals, in Prague, Czech Republic.

In addition, the values of key parameters have been modified for the analysis of one resin to evaluate their effect on morphological properties derived and to determine the optimal values for each one of them.

### 4.1. COMPARISON OF THE VALUES BETWEEN EXPERIMENTS OF THE SAME RESIN

The resin chosen for evaluating the reproducibility of the analysis was A35. To measure the reproducibility, the following formula has been used to calculate the standard error in the comparison:

$$Er = \sqrt{\frac{1}{N-1} \cdot \sum_{i=1}^N (y_i - \bar{y})^2} \quad (9)$$

Table 4.1 gathers the values of  $V_g$ ,  $d_p$  and  $S_g$  derived from the modelling of the macroporous region for each of the 3 experiments that have been considered for evaluation and their respective standard errors for A35 resin.

**Table 4.1.** Values of macroporus region parameters for A35

|                            | A35 1st | A35 2nd | A35 3rd | Er (%) |
|----------------------------|---------|---------|---------|--------|
| $V_g$ (cm <sup>3</sup> /g) | 0.46    | 0.57    | 0.59    | 0.07   |
| $d_p$ (nm)                 | 20.34   | 19.57   | 13.26   | 3.88   |
| $S_g$ (m <sup>2</sup> /g)  | 91.0    | 115.9   | 177.2   | 44.38  |

As it can be seen in the previous table, the errors both of  $V_g$  and  $d_p$  are considerably low and so quite acceptable. But the error of  $S_g$  is a bit large, below the 65% reproducibility threshold, to consider this experiments a 100% reproducible.

In the table 4.2, there are the values of  $V_{sp}$  and  $L_{pc}$  to characterize the microporous region of each of the 3 experiments that have been considered for evaluation and their respective errors for A35 resin.

**Table 4.2.** Values of microporus region parameters for A35

|                               | A35 1st | A35 2nd | A35 3rd | Er (%) |
|-------------------------------|---------|---------|---------|--------|
| $V_{sp}$ (cm <sup>3</sup> /g) | 0.91    | 1.01    | 1.18    | 0.14   |
| $L_{pc}$ (cm/g)               | 67.8    | 95.6    | 23.3    | 36.47  |

In this case both the errors of  $V_{sp}$  and  $L_{pc}$  are more reasonable meaning that the reproducibility of the experiments in relation to the microporus region is much better.

Even though, the last results are not completely bad, there is enough evidence to believe that there is room for improvement in the making of this technique to ensure the veracity of the values obtained. In Figure 4.1 (the values of this figure can be found in Annex 1) there are the values of the volumes of the gel phase divided by the different fractions of polymer density.

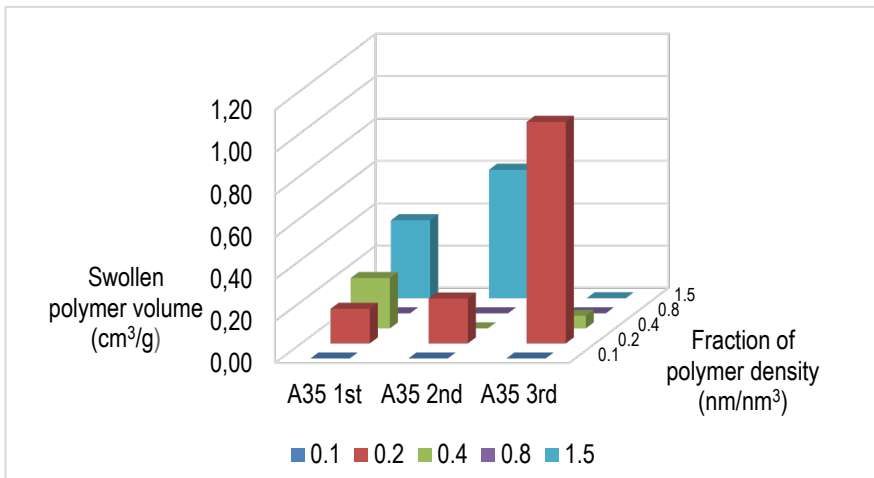


**Figure 4.1.** Comparison of the volumes in the gel phase for A35 resin

The third experiment could be considered the one that most deviates of the acceptable values, in the 1.5 and 0.2 fractions. While the first two experiments have a very similar distribution, and only being an appreciable difference in the 0.4 fraction. This leads to believe that the deviation in the previous data is caused mainly by the third experiment, and that more experiments need to be done in order to consider dismissing its results.

#### 4.2. COMPARISON OF THE VALUES BETWEEN THE EXPERIMENTS OF THIS PROJECT AND REFERENCE VALUES

For this part of the results it is needed the use of reference material in order to compare and evaluate the values obtained in the experiments done. For this purpose, data obtained by Dr. J. Guilera under the supervision of Dr. K. Jeřábek at the Institute of Chemical Process Fundamentals, in Prague, Czech Republic will be used. The values of this study will be shown next to the ones of this one and will be distinguished in their name with *ref.* (for reference). In order to evaluate the similarity between values the relative error will be calculated following the next equation:

$$E_r = \frac{E_a}{True\ value} \cdot 100 \quad (10)$$

Where the *True value* will be the one according to the reference material and  $E_a$  will be the absolute error between the reference value and the one obtained in the experiments.

In tables 4.3, 4.4, 4.5, 4.6 there are the values of  $V_g$ ,  $d_p$  and  $S_g$  to characterize the macroporous region of the resins A15, A35, A39 and CT-275, respectively both from the reference material and from the project's experiments and their error. Resin CT-124 is a micro resin, meaning that there are not permanent pores and therefore no macroporous region. Also in the case of resin A35, with which three experiments are being studied, an average will be used in order to compare the values of the three experiments with the reference ones.

**Table 4.3.** Values of macroporous region parameters for A15

|                            | A15 ref. | A15   | Er (%) |
|----------------------------|----------|-------|--------|
| $V_g$ (cm <sup>3</sup> /g) | 0.61     | 0.58  | 5.44   |
| $d_p$ (nm)                 | 15.1     | 16.7  | 10.60  |
| $S_g$ (m <sup>2</sup> /g)  | 161.6    | 138.6 | 14.22  |

**Table 4.4.** Values of macroporus region parameters for A35

|                            | A35 ref. | A35 m | Er (%) |
|----------------------------|----------|-------|--------|
| $V_g$ (cm <sup>3</sup> /g) | 0.63     | 0.54  | 14.29  |
| $d_p$ (nm)                 | 12.4     | 17.7  | 42.93  |
| $S_g$ (m <sup>2</sup> /g)  | 203.7    | 128.0 | 37.16  |

**Table 4.5.** Values of macroporus region parameters for A39

|                            | A39 ref. | A39   | Er (%) |
|----------------------------|----------|-------|--------|
| $V_g$ (cm <sup>3</sup> /g) | 0.54     | 0.29  | 46.40  |
| $d_p$ (nm)                 | 8.9      | 9.8   | 9.43   |
| $S_g$ (m <sup>2</sup> /g)  | 242.7    | 119.3 | 50.85  |

**Table 4.6.** Values of macroporus region parameters for CT-275

|                            | CT-275 ref. | CT-275 | Er (%) |
|----------------------------|-------------|--------|--------|
| $V_g$ (cm <sup>3</sup> /g) | 0.93        | 0.81   | 12.43  |
| $d_p$ (nm)                 | 18.8        | 28.8   | 21.11  |
| $S_g$ (m <sup>2</sup> /g)  | 196.7       | 143.1  | 27.25  |

As it can be seen in the previous tables the best characterizations of the macroporus regions are the ones from the resins A15 and CT-275, with not any error surpassing 30% (above 65% reproducibility). For the other two resins, A35 and A39, there is at least two of the parameters with and error above 30%, in the case of A35 the value of  $d_p$  and  $S_g$  and for A39  $V_g$  and  $S_g$ . Also is interesting to note that in all of the resins the value that diverts the most (except in the case of A39) from the reference values is the cumulative surface area, this could be related to an error/difference in the way the resin is packed into the chromatographic columns. Comparing the methods used between this project and the one done to obtain the reference values could help shed light into this issue.

In tables 4.7, 4.8, 4.9, 4.10 and 4.11 the values of  $V_{sp}$  and  $L_{pc}$  of the reference data and the ones obtained in the experiments and the error between them can be found. In this case CT-124 will be evaluated as gel-type resins are made completely of a microporus region.

**Table 4.7.** Values of microporus region parameters for A15

|                               | A15 ref. | A15  | Er (%) |
|-------------------------------|----------|------|--------|
| $V_{sp}$ (cm <sup>3</sup> /g) | 0.77     | 0.95 | 24.20  |
| $L_{pc}$ (cm/g)               | 94.2     | 56.0 | 40.56  |

**Table 4.8.** Values of microporus region parameters for A35

|                               | A35 ref. | A35 m | Er (%) |
|-------------------------------|----------|-------|--------|
| $V_{sp}$ (cm <sup>3</sup> /g) | 0.61     | 1.03  | 70.80  |
| $L_{pc}$ (cm/g)               | 65.0     | 62.2  | 4.26   |

**Table 4.9.** Values of microporus region parameters for A39

|                               | A39 ref. | A39  | Er (%) |
|-------------------------------|----------|------|--------|
| $V_{sp}$ (cm <sup>3</sup> /g) | 1.22     | 1.75 | 43.84  |
| $L_{pc}$ (cm/g)               | 121.3    | 66.7 | 45.01  |

**Table 4.9.** Values of microporus region parameters for CT-124

|                               | CT-124 ref. | CT-124 | Er (%) |
|-------------------------------|-------------|--------|--------|
| $V_{sp}$ (cm <sup>3</sup> /g) | 1.90        | 2.08   | 9.77   |
| $L_{pc}$ (cm/g)               | 120.2       | 115.1  | 4.23   |

**Table 4.10.** Values of microporus region parameters for CT-275

|                               | CT-275 ref. | CT-275 | Er (%) |
|-------------------------------|-------------|--------|--------|
| $V_{sp}$ (cm <sup>3</sup> /g) | 0.85        | 1.12   | 31.76  |
| $L_{pc}$ (cm/g)               | 76.3        | 20.4   | 73.32  |

Also to evaluate the microporus region in Figure 4.2 (the values of this figure can be found in Annex 1) there are represented the values of the volumes of the gel phase divided by the different fractions of polymer density of the five resins, both reference data and the ones of this project in order to visualize the reproducibility of the results.

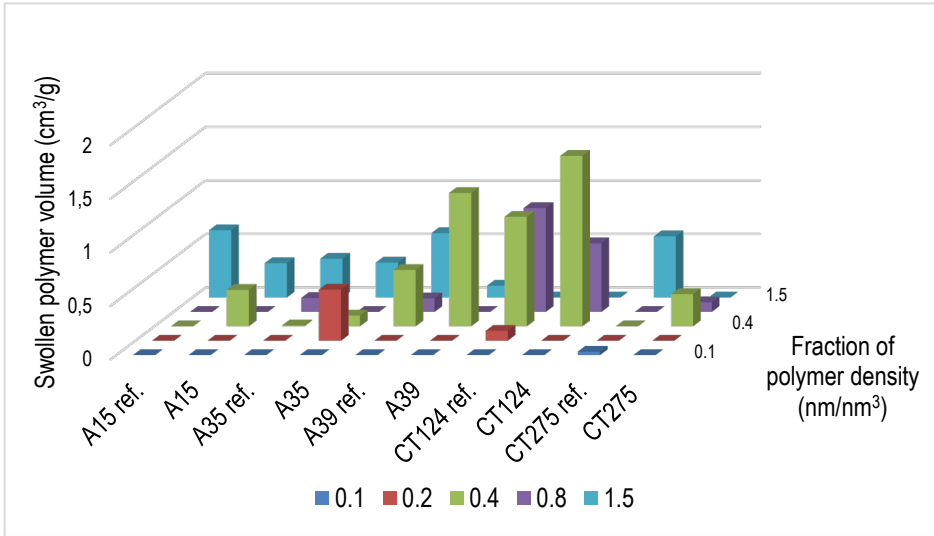


**Figure 4.2.** Comparison of the volumes in the gel phase for the reference data and the experimental data for each resin

In the evolution of the gel phase region between the reference material and the experimental values there are a few subjects to address for each resin.

For A15 the value of the errors for the  $V_{sp}$  and  $L_{pc}$  values, are high, but only the  $V_{sp}$  is inside the limit of 65% of reproducibility. Then looking at Figure 4.2 there are major differences in the distribution of the polymer density, while in the reference material there is only in 1.5 nm/nm<sup>3</sup> fraction in the experiment values there are at 0.4 and 1.5 nm/nm<sup>3</sup> values and 1.5 nm/nm<sup>3</sup> fraction has a lower value than in the reference data.

For A35 the error of  $V_{sp}$  is too high, 70.80% to consider a viable reproducibility between the reference material and the one obtained in the experiments for the microporus region. Also in the distribution of the polymer density (see Figure 4.2) although the predominant fraction is in both cases 1.5 nm/nm<sup>3</sup>, in the reference data the other predominant fraction is 0.8 nm/nm<sup>3</sup>, while in the experimental data is the 0.2 nm/nm<sup>3</sup>.



For A39 both the error of  $V_{sp}$  and  $L_{pc}$  are above 40% which means that the reproducibility of this experiments is not good enough. In Figure 4.2 there are clear differences while A39 reference data the dominant fraction is by a very little margin 1.5 nm/nm<sup>3</sup> over 0.4 nm/nm<sup>3</sup> in the experimental values the 0.4 nm/nm<sup>3</sup> fraction is much bigger than 1.5 nm/nm<sup>3</sup> fraction.

For CT-124 both  $V_{sp}$  and  $L_{pc}$  values have very little error between the data of reference and the experimental one. And in the figure 4.2 both the reference data and the experimental data have the same dominant fractions 0.4 nm/nm<sup>3</sup> and 0.8 nm/nm<sup>3</sup>, but in the experimental there is a much bigger difference between the two values, unlike the reference data were the value of the fraction is quite similar. Nevertheless, this resin is very well characterize and the differences between the results of this project and the reference ones are quite small.

Finally for CT-275 the value of the error of  $L_{pc}$  is too large to consider that there is similarity between the reference data and the experimental one. Also in the figure 4.2 from the reference data it is clear that the dominant fraction is 1.5 nm/nm<sup>3</sup>, whereas in the experimental data the dominant one is 0.4 nm/nm<sup>3</sup>.

Combining both the information of the macroporus and microporus region, it can be extracted that the only resin that has been completely characterize with minimal error is the CT-124 resin and that from the rest A15, A35 and A39 are the ones that although not completely similar have enough similarities to think that with a few more experiments more conclusive results could have been achieved.

### **4.3. EVALUTION OF THE EFFECT CHANGES IN PARAMETERS: KINETIC DIAMETER, MACROPORE LIMIT AND CHIAN DIAMETER TO THE EXPERIMENTAL CHACARTERIZATION OF RESINS**

As explained, to characterize the morphological properties of the resins a combination of methods by the Ogston model and the cylindrical pore model is used. There are three important parameters used in the modelling whose values have been set to those suggested by K. Jeřábek as the optimum ones. From his studies he has established that the macropore limit is set at 10.22 nm, the polymeric chain diameter is 0.4 nm and that kinetic diameter or kinetic diameter is 2. However, it is interesting to vary these values to assess how they influence the resulting morphological properties from the analysis.

In this part of the results two experiments will be analysed modifying the value of these parameters to: macropore limit to 8 polymeric chain diameter from 0.3 to 0.5 and kinetic diameter from 1.5 to 2.5. And later evaluate the changes that have been caused to the characterization of the resin.

In the table 4.12 are the values of  $V_g$ ,  $d_p$ ,  $S_g$ ,  $V_{sp}$  and  $L_{pc}$ , respectively for each changed parameter, and are put in comparison with the A35 resin values without the modified parameters.

**Table 4.12.** Variation of values of parameters for A35

|          | Standard | L=1.5  | L=2.5  | $d_c=0.3$ | $d_c=0.5$ | Macro. Limit 8 |
|----------|----------|--------|--------|-----------|-----------|----------------|
| $V_g$    | 0.463    | 0.460  | 0.455  | 0.463     | 0.463     | 0.463          |
| $d_p$    | 20.339   | 20.559 | 20.670 | 20.339    | 20.339    | 20.339         |
| $S_g$    | 90.967   | 89.510 | 88.033 | 90.967    | 90.967    | 90.967         |
| $V_{sp}$ | 0.905    | 0.908  | 0.913  | 0.905     | 0.905     | 0.905          |
| $L_{pc}$ | 67.788   | 67.917 | 68.514 | 62.525    | 74.661    | 67.788         |

In the table 4.12, the first three rows of data ( $V_g$ ,  $d_c$  and  $S_g$ ) are for the macroporus region. It can be observed that there is no influence from the polymeric chain diameter nor from the macropore limit with the parameters, but the kinetic diameter does appear to modify the values of  $V_g$ ,  $d_p$  and  $S_g$  (see Figure 4.3, the values of this figure can be found in Annex 1).

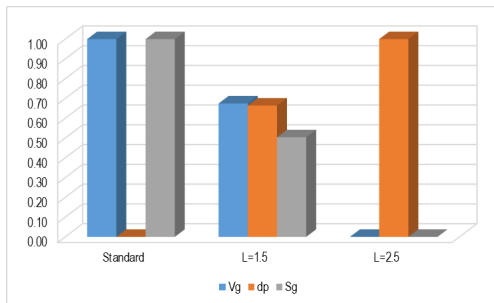


**Figure 4.3.** Comparison of the normalized values of the macroporus region parameters under the influence of the kinetic diameter for A35 resin

It appears that the kinetic diameter is chosen in order to minimize the pore diameter and maximize the cumulative surface area and the cumulative pore volume.

In the microporous region (Table 4.12 the  $V_{sp}$  and  $L_{pc}$  rows) the macropore limit still does not affect the values of the parameters, but both the polymeric chain diameter and kinetic diameter do. Both polymeric chain diameter and kinetic diameter seem to be directly proportional to the total length of polymer chains while only the kinetic diameter seems to influence true swollen polymer volume. In this case K. Jeřábek has taken the parameter value that minimizes the value of the true swollen polymer volume.

#### 4.4. ASSESSMENT OF THE RELATIONSHIP BETWEEN CATALYTIC ACTIVITY AND MORPHOLOGICAL PROPERTIES

One of the most important applications of the characterization results obtained by ISEC is to correlate them with the catalytic activity observed in a chemical reaction system. It is well known that the amount of sulfonic groups present in a resin is key to its catalytic activity, but accessibility it is as well important. To determine which variables represent better the relation between the catalytic activity and the morphological properties, the response surface methodology was used in previous studies for the etherification reactions to produce ETBE and TAEE. It was obtained that the catalytic activity of IERs can be directly related to the ratio  $H^+/V_{sp}$  [27], showing a linear trend [27]. From this result, it can be deduced resins with high acid capacity in a small volume of swollen polymer can allow cluster formation or coordination of active sites that eventually boost etherification reaction rates.

As discussed previously, significant differences in terms of ISEC results emerged from the comparison of our values with those from the reference lab. However, it is still worthy to assess how our results can be correlated to catalytic activity and how they do compare to those derived from the correlation with the reference lab ones. Figure 4.4 (the values of this figure can be found in Annex 1) shows the relation between the ETBE production reaction rates vs. the ratio  $H^+/V_{sp}$  derived from the use our  $V_{sp}$  values and those from the reference lab. As it can be seen, in both cases the catalytic activity increased with an increase in the ratio  $H^+/V_{sp}$ . This is a satisfactory result since indicates that even though the observed differences in terms of the parameters magnitude, our values are able to show the correlation between catalytic activity and

morphological properties of the resins. The differences in the slope can be ascribed to the differences in the parameters magnitude between our values and those from the reference lab.

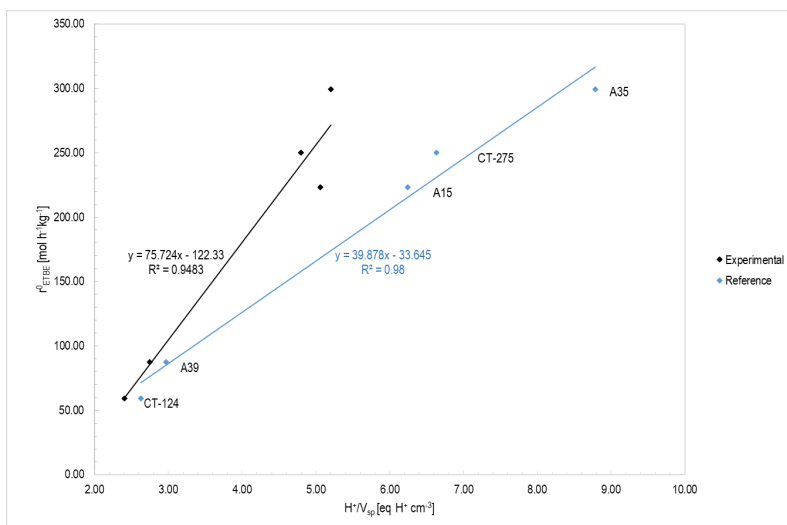


**Figure 4.4.**  $r_i^0$  in front of ratio of acid capacity to volume of the swollen polymer for reference and experimental data

## 5. CONCLUSIONS

The ISEC technique implementation at the laboratory of Applied Kinetics and Catalysis in the University of Barcelona has been achieved. However, an improvement is still necessary to refine it and obtain more reliable and reproducible results.

A column packing methodology using the wet filling technique has been developed during this project, but there is still a few adjustments to do because some of the experiments had to be restarted because the column was not correctly packed (observing the pressure values). Even the experiment was apparently successful, there is always some degree of discrepancy with the weight of the resin that was packed and with the total balance of the column volume.

CT-124 resin has been characterized with an excellent reproducibility in comparison to the reference data.

A15, A35, A39 and CT-275 resins have not been able to properly characterized in comparison to the reference data and more experiments should be done. Although in the case of A15 and A35 there were clear similarities in the distribution of fraction of polymer density.

There are correlations between the parameters used by K. Jeřábek for the calculation of the ISEC technique and key morphological variables, which would require a deeper research in those parameters to find their optimal value. In the case of the kinetic diameter it seems the objective is to minimize the pore diameter and the swollen polymer volume. The polymeric chain diameter is directly proportional to the total length of polymer chains. And finally the macropore limit does not seem to have any significant effect on the variability of the chosen parameters.

In the assessment of the catalytic activity from the results of this project and from the reference material it can be seen that the catalytic activity increases with an increase in the ratio  $H^+/V_{sp}$ .

The  $H^+/V_{sp}$  ratio proves that even though some of the characterizations have some errors they are not completely wrong, because the order of the resins in the catalytic behaviour is the same as the reference data.

Comparing the data, the best results are the ones from the CT-124 and A39 resins, while A15, A35 and CT-275 show more discrepancy.

---

Finally, I believe that the key factor that will effect largely to the future of the usage of the ISEC technic in the University of Barcelona is to improve and standardise the column packing. For example using a chromatographic column for ISEC with a larger internal diameter and the utilization of a vacuum system.

## REFERENCES AND NOTES

1. Soto, R. Simultaneous etherification of C<sub>4</sub> and C<sub>5</sub> iso-olefins with ethanol over acidic ion-exchange resins for greener fuels (PhD Thesis). University of Barcelona, Barcelona. (2017).
2. The Trouble with Lithium 2. Meridian International Research. 2008.
3. The Precious Mobile Metal. Credit Suisse. 2014.
4. J. Burri, R. Crockett, R. Hany, D. Rentsch. Gasoline composition determined by <sup>1</sup>H NMR spectroscopy. *Fuel*. 83 (2004) 187–193.
5. R. da Silva, R. Cataluña, E. W. de Menezes, D. Samios, C. M. S. Piatnicki. Effect of additives on the antiknock properties and Reid vapor pressure of gasoline. *Fuel*. 84 (2005) 951–959.
6. M. Lebreton. Hot and cold fuel volatility indexes of French cars: a cooperative study by the GFC Volatility Group. SAE Tech. Pap. 841386 (1984).
7. A. Arteconi, A. Mazzarini, G. Nicola. Emissions from ethers and organic carbonate fuel additives: a review. *Water, Air, Soil Pollut.* 221 (2011) 405–423.
8. T. Higgins and P. Steiner. Study on relative CO<sub>2</sub> savings comparing ethanol and TAAE as a gasoline component. Hart energy consulting, 2010.
9. R. Cascone. Biobutanol-a replacement for bioethanol?. *Chem. Eng. Prog.* 108 (2008) 54–59.
10. T. Dođü, D. Varisli. Alcohols as Alternatives to Petroleum for Environmentally Clean Fuels and Petrochemicals. *Turkish J. Chem.* 31 (2007) 551–567.
11. San Francisco Bay Area Regional Water Quality Control Board Integrated Basin Management Plan (2004).
12. R. K. Niven. Ethanol in gasoline: environmental impacts and sustainability review article. *Renew. Sustain. Energy Rev.* 9 (2005) 535–555.
13. D. Pimentel, T. Patzek, G. Cecil. Ethanol production: energy, economic, and environmental losses. *Rev. Environ. Contam. Toxicol.* (2007) 25–41.
14. H. L. Brockwell, P. R. Sarathy, R. Trotta. Synthesize ethers. *Hydrocarb. Process.* 70 (1991) 133–141.
15. González Sánchez, R. Performance of Amberlyst™35 in the synthesis of ETBE from ethanol and C<sub>4</sub> cuts. (PhD Thesis). University of Barcelona, Barcelona (2011).
16. Corain, Benedetto & Zecca, M & Jerábek, Karel. Catalysis and polymer networks - The role of morphology and molecular accessibility. *Journal of Molecular Catalysis A-chemical - J MOL CATAL A-CHEM.* (2001). 177. 3-20.
17. Lee, B; Richards, FM. "The interpretation of protein structures: estimation of static accessibility". *J Mol Biol.* (1971). 55 (3): 379–400
18. Jeřábek K. Inverse Steric Exclusion Chromatography as a Tool for Morphology Characterization. 1996 [cited May 2019]. p. 211–24.
19. Jeřábek K. Determination of pore volume distribution from size exclusion chromatography data. *Anal Chem [Internet]. American Chemical Society; 1985 Jul [cited May 2019];57(8):1595–7.*
20. Jeřábek K. Characterization of swollen polymer gels using size exclusion chromatography. *Anal Chem [Internet]. American Chemical Society; 1985 Jul [cited May 2019];57(8):1598–602.*
21. R.H. Grubs, E.M. Sweet, *Macromolecules* 8 (1975) 241.
22. K.S. Ro, S.I. Woo, *J. Mol. Catal.* 61 (1990) 27.
23. A.M. Hecht, R. Duplessix, E. Geissler, *Macromolecules* 18 (1985) 2167.
24. G.C. Rex, S. Schlick, *J. Phys. Chem.* 89 (1985) 3598.
25. W.T. Ford, M. Periasamy, *Macromolecules* 17 (1984) 2881.

- 
26. M. Tomoi, W.T. Ford, *J. Am. Chem. Soc.* 103 (1981) 3828.
  27. Soto, Rodrigo & Fité, Carles & Ramírez, Eliana & Iborra, Montserrat & Tejero, Javier. Catalytic activity dependence on morphological properties of acidic ion-exchange resins for the simultaneous ETBE and TAAE liquid-phase synthesis. *Reaction Chemistry & Engineering*. (2018). 3, 195–205.



## ACRONYMS

BP: British Petroleum

GHG: Greenhouse gases

LPG: Liquefied petroleum gas

LNG: Liquefied natural gas

US: United States

CO<sub>2</sub>: Carbon dioxide

NO<sub>2</sub>: Nitrogen dioxide

PM: Particulate Matter

VOC: Volatile organic compound

CO: Carbon monoxide

PM<sub>10</sub>: Particulate Matter of 10 or less micrometres

PM<sub>2.5</sub>: Particulate Matter of 2.5 or less micrometres

PM<sub>0.1</sub>: Particulate Matter of 0.1 or less micrometres

NO<sub>x</sub>: Nitrogen oxides

PANs: Peroxyacyl nitrates

bRVP: blending Reid vapour pressure

CAAA: Clean Air Act Amendments

FFV: Flexible Fuel Vehicles

MBTE: Methyl *tert*-butyl ether

ETBE: Ethyl *tert*-butyl ether

TAME: *Tert*-amyl methyl ether

TAAE: *Tert*-amyl ethyl ether

EtOH: Ethanol

FCC: Fluid catalytic cracking  
SC: Steam cracking  
K: Kelvin (temperature)  
IER: Ion-exchange resin  
PS-DVB: Polystyrene-divinylbenze  
DVB: Divinylbenze  
nm: Nanometre  
N<sub>2</sub>: Nitrogen gas  
BET: Brunauer–Emmett–Teller  
ISEC: Inverse steric exclusion chromatography  
V<sub>e,j</sub>: Elution volume of a solute j  
V<sub>0</sub>: dead volume of a chromatographic column  
K<sub>j</sub>: Partition constant of solute j  
V<sub>p</sub>: Pore volume  
d<sub>p</sub>: pore characteristic dimension  
L: dimension characteristic  
K<sub>c</sub>: Partition constant of solute j for the cylindrical pore model  
K<sub>o</sub>: Partition constant of solute j for the Ogston model  
C: Chain density of the gel phase  
d<sub>s</sub>: molecule spherical diameter  
ESR: Electron Spin Resonance  
NMR: Nuclear magnetic resonance  
XRMA: X-Ray Micro-Analysis  
N: equivalent concentration  
rpm: Revolutions per minute  
HPLC: High Performance Liquid Chromatography  
mL: millilitre  
MW: Molecular weight

USA: United States of America

eq H<sup>+</sup>: Equivalent weight

°C: Centigrade (temperature)

Min: Minute

RID: Refractive Index Detector

d<sub>column</sub>: Internal chromatographic column diameter

μL: Microlitre

Na<sub>2</sub>SO<sub>4</sub>: Sodium sulphate

t<sub>r</sub>: Retention time

Excel: Microsoft Office Excel®

V<sub>g</sub>: Cumulative Pore Volume

S<sub>g</sub>: Cumulative Surface Area

V<sub>sp</sub>: True swollen polymer volume

L<sub>pc</sub>: Total length of polymer chain



# APPENDICES



## APPENDIX 1: VALUES FOR FIGURES

Values for Figure 4.1

|         | 0.1  | 0.2  | 0.4  | 0.8  | 1.5  |
|---------|------|------|------|------|------|
| A35 1st | 0.00 | 0.16 | 0.24 | 0.00 | 0.37 |
| A35 2nd | 0.00 | 0.15 | 0.43 | 0.00 | 0.10 |
| A35 3rd | 0.00 | 0.21 | 0.00 | 0.00 | 0.61 |

Values for Figure 4.2

|             | 0.1  | 0.2  | 0.4  | 0.8  | 1.5  |
|-------------|------|------|------|------|------|
| A15 ref.    | 0.00 | 0.00 | 0.00 | 0.00 | 0.63 |
| A15         | 0.00 | 0.00 | 0.34 | 0.00 | 0.32 |
| A35 ref.    | 0.00 | 0.00 | 0.01 | 0.13 | 0.36 |
| A35         | 0.00 | 0.18 | 0.22 | 0.00 | 0.35 |
| A39 ref.    | 0.00 | 0.00 | 0.53 | 0.13 | 0.60 |
| A39         | 0.00 | 0.00 | 1.24 | 0.00 | 0.11 |
| CT-124 ref. | 0.00 | 0.09 | 1.02 | 0.97 | 0.00 |
| CT-124      | 0.00 | 0.00 | 1.59 | 0.64 | 0.00 |
| CT-275 ref. | 0.03 | 0.00 | 0.00 | 0.00 | 0.57 |
| CT-275      | 0.00 | 0.00 | 0.30 | 0.09 | 0.00 |

Values for Figure 4.3

|             | 0.1  | 0.2  | 0.4  | 0.8  | 1.5  |
|-------------|------|------|------|------|------|
| A15         | 0.00 | 0.00 | 0.34 | 0.00 | 0.32 |
| A15 (d=0.3) | 0.00 | 0.00 | 0.29 | 0.00 | 0.31 |
| A15 (d=0.5) | 0.00 | 0.00 | 0.54 | 0.00 | 0.45 |
| A15 (L=1.5) | 0.00 | 0.00 | 0.33 | 0.00 | 0.32 |
| A15 (L=2.5) | 0.00 | 0.00 | 0.34 | 0.00 | 0.32 |

Values for Figure 4.4

|        | $r_{ETBE}^0$ * | Acid Capacity <sup>†</sup> | $V_{sp}$ | $H^+/V_{sp}$ | $V_{sp,ref}$ | $H^+/V_{sp,ref}$ |
|--------|----------------|----------------------------|----------|--------------|--------------|------------------|
| A15    | 223.30         | 4.81                       | 0.97     | 4.96         | 0.77         | 6.25             |
| A35    | 299.53         | 5.36                       | 0.95     | 5.64         | 0.61         | 8.79             |
| A39    | 87.25          | 4.81                       | 1.75     | 2.75         | 1.62         | 2.97             |
| CT-124 | 58.97          | 5.00                       | 2.08     | 2.40         | 1.90         | 2.63             |
| CT-275 | 249.97         | 5.37                       | 1.12     | 4.79         | 0.81         | 6.63             |

\*[28] Data from R. Soto et al., *React. Chem. Eng.*, 2018, 3, 195–205





